Disruptions in global network segregation and integration in adolescents and young adults with Fetal Alcohol Spectrum Disorder

Carlos I. Rodriguez, Ph.D.[1], Victor Vergara, Ph.D.[2], Vince Calhoun, Ph.D.[2], Daniel D. Savage, Ph.D.[3,4], Derek A. Hamilton, Ph.D. [3,4], Claudia D. Tesche, Ph.D.[4], Julia M. Stephen, Ph.D. [1]

Affiliations

1. The Mind Research Network. 1101 Yale Blvd. NE, Albuquerque, NM, 87106, USA.
2. Tri-Institutional Center for Translational Research in Neuroimaging and Data Science (TReNDS), Georgia State University, Georgia Institute of Technology, and Emory University. 55 Park Pl NE, Atlanta, GA 30303, USA.
3. Department of Neurosciences, University of New Mexico School of Medicine. 1 University of New Mexico, Albuquerque, NM, 87131, USA.
4. Department of Psychology, University of New Mexico. 1 University of New Mexico, Albuquerque, NM 87131, USA.

Running Title: Brain network disruptions in FASD

Corresponding Author:

Carlos I. Rodriguez
The Mind Research Network
1101 Yale Boulevard Northeast

Albuquerque, NM 87106

Phone: 505-301-5483

Email: crodriguez@mrn.org

Keywords: Prenatal Alcohol Exposure, Fetal Alcohol Spectrum Disorder, Graph Theory, Functional Network Connectivity, functional MRI (fMRI)

Abstract

Background: Fetal Alcohol Spectrum Disorder (FASD) represents a significant public health concern that is associated with a broad range of physical, neurocognitive, and behavioral effects associated with prenatal alcohol exposure (PAE). Magnetic resonance imaging (MRI) has been an important tool for advancing our knowledge of abnormal brain structure and function in individuals with FASD. However, only a small number of studies have applied graph theory-based network analysis to resting state functional MRI (fMRI) data in individuals with FASD highlighting a need for additional research in this area.

Methods: Resting state fMRI data were collected from adolescent and young adult participants (ages 12-22) with Fetal Alcohol Syndrome (FAS) or alcohol related neurodevelopmental disorder (ARND) and neurotypically-developing controls (CNTRL) from previous studies. Group independent components analysis (gICA) was applied to fMRI data to extract components representing functional brain networks. Functional network connectivity (FNC), measured by Pearson correlation of the average independent component (IC) time series, were analyzed under a graph theory framework to compare network modularity, the average clustering coefficient, characteristic path length, and global efficiency between groups. Cognitive intelligence, measured by the Wechsler Abbreviated Scale of Intelligence (WASI), was correlated to global network measures.

Results: Group comparisons revealed significant differences in the average clustering coefficient, characteristic path length, and global efficiency. Modularity was not significantly different between groups. The FAS and ARND groups scored significantly lower in Full Scale IQ (FS-IQ) and the Vocabulary subtest, but not the Matrix Reasoning subtest when compared to the CNTRL group. No significant associations between intelligence and graph theory measures were detected.

Conclusion: Our results partially agree with previous studies examining global graph theory metrics in children and adolescents with FASD and suggest that exposure to alcohol during prenatal development leads to disruptions in aspects of functional network segregation and integration.

Introduction

Fetal Alcohol Spectrum Disorder (FASD) describes a long-lasting and broad range of physical, neurocognitive, and behavioral effects caused by exposure to alcohol during prenatal development (Sokol et al., 2003). The term FASD encompasses several diagnostic labels that range in severity and include Fetal Alcohol Syndrome (FAS), partial fetal alcohol syndrome (pFAS), and alcohol related neurodevelopmental disorder (ARND). Individuals with FAS have characteristic facial dysmorphology and growth restrictions, whereas individuals with pFAS exhibit some, but not all, of the characteristics linked to FAS. Individuals with ARND have confirmed prenatal alcohol exposure (PAE) with cognitive and behavioral effects but lack the dysmorphic features observed in FAS. In the United States, the estimated prevalence rate of FASD falls between 1.1% and 5.0% of children (May et al., 2014, May et al., 2018), which designates FASD as a leading preventable cause of neurodevelopmental disorders.

Research utilizing magnetic resonance imaging (MRI) has demonstrated that PAE is linked to several abnormalities in brain structure that include reductions in brain volume (microcephaly) (Coles et al., 2011, Chen et al., 2012), impaired development of the corpus callosum (Astley et al., 2009, Riley et al., 1995), changes in white matter organization (Ma et al., 2005, Long et al., 2020, Wozniak et al., 2009), abnormal cortical thickness (Yang et al., 2012, Zhou et al., 2011), and reduced cerebellar volume (Coles et al., 2011). A complementary body of research employing functional MRI (fMRI) has demonstrated impaired brain function during tasks that assess working memory (Malisza et al., 2005), response inhibition (Fryer et al., 2007), number processing (Meintjes et al., 2010), and arithmetic processing (Santhanam et al., 2009).

Studies relying on resting state fMRI using seed-based and ICA-based connectivity analyses, have associated PAE to alterations in functional connectivity of the default mode network (DMN) (Santhanam et al., 2011), salience, attention, executive, (Fan et al., 2017), sensorimotor (Long et al., 2018), frontal-parietal, and language networks (Little et al., 2018), along with impaired interhemispheric transfer (Wozniak et al., 2011). Whole brain resting state functional connectivity data from individuals exposed to prenatal alcohol and neurotypically-developing controls have also been compared within a graph theoretical framework.

In graph theory, networks are mathematically represented as systems consisting of interconnected elements known as nodes and edges (Sporns, 2011, Fornito et al., 2016). In the context of fMRI data, nodes can represent voxels or groups of voxels, while edges can represent the functional connectivity between nodes. Several measures of network properties are available, many of which describe functional network segregation and integration. Measures of network segregation quantify the extent to which networks organize into densely coupled clusters or modules that support specialized processing and include modularity and the average clustering coefficient (Sporns, 2011). On the other hand, measures of network integration, such as the characteristic path length and global efficiency, capture the extent to which networks engage in global interactions by combining specialized information from distributed nodes (Sporns, 2011, Rubinov and Sporns, 2010).

Currently, only a small number of studies have applied network analysis to resting state fMRI data acquired from individuals exposed to alcohol prenatally with mixed results. In a study of children ages 2-7, no significant differences in multiple network measures such as the clustering coefficient, global efficiency, and path length, were detected between neurotypically-developing controls and those with PAE (Long et al., 2019). Similarly, in a large, multi-site sample of children and adolescents ages 7-17, no significant differences between PAE and neurotypically-developing controls were reported in network measures such as the characteristic path length, average clustering coefficient, and global efficiency, although abnormal patterns of connectivity were more common in the PAE group when compared to controls (Wozniak et al., 2017). In a sample of children and adolescents aged 10-17, PAE was associated with significant increases in characteristic path length and reductions in global efficiency relative to controls, suggesting abnormal network integration (Wozniak et al., 2013). While, the two Wozniak et al., studies relied on the same regions of interest, they differed slightly in their graph construction approaches, and the multi-site data in the Wozniak et al., 2017 study were acquired from multiple MR scanner manufacturers using different image acquisition parameters.

Each of the aforementioned studies relied on seed-based nodal definition schemes in which regions of interest (ROIs) were selected *a priori*. Furthermore, the previous studies performed network analysis on binarized graphs which only describe the presence or absence of connections rather than connection strength described by weighted graphs. Taken together, these considerations highlight the need for additional research with alternative, yet equally important, methods for network definition schemes and graph construction approaches in an effort to gain a more complete understanding of the effects of PAE on network integration and segregation.

To address these gaps in the literature, the present study utilized spatial group independent components analysis (gICA) of resting state fMRI data gathered from adolescents and neurotypically-developing controls. As a data driven technique, spatial group ICA identifies sets of voxels with common features in patterns of brain activation without the need to define *a priori* regions of interest. Network properties were then computed from weighted graphs constructed from pairwise correlations between the average time series of independent components (ICs). Finally, we associated graph theory metrics to cognitive intelligence as measured by the Wechsler's Abbreviated Scale of Intelligence (WASI) (Wechsler, 2009). Given that previous research demonstrated a pattern of reduced network connectivity in older children, we predicted to observe decreases in network connectivity as a result of PAE. In addition, we expected decreases in network connectivity to be associated with cognitive intelligence in PAE participants.

Methods

Participants

Data from fifty-eight male and female adolescent and young adult participants (aged 12-22) were previously recruited from urban and rural New Mexico as part of separate studies (Coffman et al., 2013, Tesche et al., 2015, Vakhtin et al., 2015) and pooled for the present investigation. Participants with FASD were evaluated by a multidisciplinary team which included a clinical psychologist, a neuropsychologist and a pediatrician trained in FAS-related dysmorphology at the University of New Mexico's Fetal Alcohol Diagnostic and Evaluation Clinic under the modified Institute of Medicine (IOM) criteria (Hoyme et al., 2005) as these data were collected in 2011,before the development of newer diagnostic systems. To summarize these criteria, a diagnosis of FAS (n=13) resulted from evidence of facial dysmorphologies, growth retardation, central nervous system abnormalities, with or without confirmed maternal alcohol exposure, and cognitive-behavioral effects inconsistent with developmental stage. A diagnosis of pFAS (n=1) resulted from confirmed maternal alcohol exposure, evidence of some of the facial characteristics of FAS and evidence of either growth retardation, central nervous system abnormalities, or a pattern of cognition or behavior that is inconsistent with developmental stage that could not be explained by other familial background or environmental factors. Finally, a diagnosis of ARND (n=8) resulted from evidence of central nervous system abnormalities and/or a cognitive-behavioral pattern inconsistent with developmental stage that could not be explained by other familial background or environmental factors. Because only one participant was diagnosed with pFAS, that participant was recoded as ARND for statistical analyses based on a Full Scale-Intelligence Quotient (FS-IQ) score (FS-IQ=101) that was more similar to the mean of the ARND group than that of the FAS group. For participants with FASD, maternal alcohol consumption was determined either by direct confirmation during maternal interview, eye witness reports of maternal drinking during pregnancy, or via legal records confirming alcohol consumption during pregnancy (e.g. DWI arrest). Since participants were recruited in the 12-22 year age-range, retrospective estimates of PAE from mothers or caregivers were not obtained. Healthy controls (CNTRL, n=36) had no evidence of prenatal exposure to any substances and had no history of developmental, neurological, or psychological conditions as assessed by caregiver interview. Data collection protocols were approved by the Human Research Review Committee of the University of New Mexico Health Sciences Center. Informed consent by participants or caregivers (if subject was under the age of 18) was provided in accordance with institutional guidelines. Group sample sizes reflect the remaining participants after excluding those with severe signal drop out during MRI scan or that surpassed three standard deviations away from the mean in measures of head motion using framewise displacement (FD) (Power et al., 2012).

MRI Data Acquisition

All MRI data were gathered at the Mind Research Network (MRN; Albuquerque, NM) using a Siemens Trio 3-Tesla scanner with a 12-channel radio frequency coil. Structural T1-weighted MR images were obtained with a multiecho 3D MPRAGE sequence [FOV=256mm x 256mm, matrix=256 x 256, TE=1.64, 3.5, 5.36, 7.22, 9.08 ms, TR=2530ms, TI=1200 ms, flip angle=7˚, number of excitations=1, slice thickness=1mm, and 192 slices]. Depending on the sample, functional T2*-weighted MRI images were obtained during a 5- or 5.5-minute resting state scan with a gradient-echo EPI sequence [FOV=240mm x 240mm, matrix=64 x 64, voxel size=3.75mm x 3.75mm x 4.55mm, TR=2000ms, TE=29ms, flip angle=75˚, slice thickness=3.55 mm, slice gap=1.05 mm]. Only the first 300 timepoints (5 minutes) of each participant's functional scan were used for subsequent data processing and analyses.

Functional MRI data preprocessing

fMRI data were partly pre-processed using an automated pipeline consisting of realignment, slice-time correction, normalization to the Montreal Neurological Institute (MNI) space, and resampling to 3mm^3 voxels with the Statistical Parametric Mapping 5 [SPM5, https://www.fil.ion.ucl.ac.uk/spm/, (Friston et al., 1994)] toolbox implemented in MATLAB (Mathworks, Nattick, MA). Voxelwise time-series were then despiked with the AFNI 3dDespike program (Cox, 1996), and regressed for motion using a 12 parameter model (6 parameters derived from the realignment procedure and their derivatives). Images were then smoothed in SPM5 with a 10mm full-width half-maximum (FWHM) Gaussian kernel to account for intersubject anatomical variability (Konrad et al., 2005).

Independent Components Analysis and Graph Construction

fMRI data were processed using the Group ICA of fMRI Toolbox (GIFT, https://trendscenter.org/software/gift) implemented in MATLAB using the INFOMAX algorithm for feature identification. As described in Allen and colleagues (2011), Group ICA was configured to extract a total of 75 ICs and 113 principal components for data reduction. Component time courses were temporally filtered using a low pass filter with a 0.15Hz frequency cut-off and all ICs were visually inspected for artifactual features including motion-related and susceptibility artifacts, spectral power characteristics, and anatomical location (e.g. white matter or ventricles) resulting in the exclusion of 32 components and yielding 43 retained components. Retained component coordinates and anatomical labels are listed in Supplementary Table 1 and visually displayed in Supplementary Figure 1. Pearson correlations between all possible pairs of the 43 retained ICs were computed as part of the GIFT output. Correlations were then remapped to connectivity weights by taking the absolute value of each correlation coefficient to include anti-correlations in the analysis (Kazeminejad and Sotero, 2020). Data for each subject consisted of a matrix that contained a total of 903 ((43*(43-1)/2) unique possible weights where, in graph theory terminology, each of the 43 components represented a node and each connectivity weight represented an edge.

Graph metrics consisted of modularity, average clustering coefficient, characteristic path length and global efficiency, all of which were computed with the Brain Connectivity Toolbox

[BCT, https://sites.google.com/site/bctnet/ (Rubinov and Sporns, 2010)] in MATLAB (Mathworks, Nattick, MA). Each subject matrix was used to construct five additional connectivity matrices that were proportion thresholded such that the top 10%, 20%, 30%, 40%, or 50% of the strongest connectivity values (edges) were retained for graph metric computation. The rationale for this approach was to ensure the resulting connectivity matrices, within each threshold, contained the same number of edges for group comparisons and to limit the influence of spurious connections (Bullmore and Bassett, 2011). Thresholds were reported in a range of 0.1 to 0.5 in increments of 0.1, where 0.1 represents the 10% proportion threshold. Thresholded connectivity matrices were utilized to measure modularity and the average clustering coefficient. Network modularity, which reflects the balance of between- and within-module connectivity, was estimated using the Newman algorithm that subdivides a network into separate modules, such that within module connections are maximized and between module connections are minimized (Newman, 2006). To describe the density and strength of connections between nodes, we utilized the weighted definition of node level clustering as proposed by (Onnela et al., 2005). The average clustering coefficient at the subject-level was then computed as the arithmetic mean of all node level clustering coefficients (Fornito et al., 2016). To measure characteristic path length and global efficiency, sets of separate subject level distance matrices were constructed by applying the inverse transform (T(x)=1/x) to each edge weight value in the connectivity matrix with the aim of representing strong connectivity values as short distances. The characteristic path length was computed as the average of the shortest path between all possible pairs of nodes (Watts and Strogatz, 1998). The global efficiency (Latora and Marchiori, 2001) of a network, which serves as an added measure of network integration, was computed as the average of the inverse of the shortest path lengths between all possible pairs of nodes (Sporns, 2011, Achard and Bullmore, 2007).

Neuropsychological Assessments

Participant’s cognitive intelligence was estimated with the two-subtest form of the Wechsler Abbreviated Scale of Intelligence (WASI) (Wechsler, 2009) comprised of Vocabulary and Matrix Reasoning subtests. The Vocabulary subtest measures word knowledge, verbal concept formation, fund of knowledge, crystallized intelligence, and degree of language development. The Matrix Reasoning subtest measures fluid and visual intelligence, spatial ability, and perceptual organization. Subtest scores were used to form a FS-IQ estimate.

Statistical Analyses

Statistical analyses were conducted in R version 4.0.0 (R Development Core Team, 2020). Measurements of motion were analyzed by comparing mean framewise displacement (FD) across the three groups (CNTRL, ARND, and FAS) using one-way analysis of variance (ANOVA). Graph theory measures were regressed for age, sex, and mean framewise displacement before comparisons in separate two-way ANOVAs. FS-IQ, Vocabulary, and Matrix Reasoning scores were compared in separate one-way ANOVAs. Effect sizes are reported as partial eta squared (η^2_p) for ANOVA tests and as Hedge’s g_s for between-group comparisons. FS-IQ estimates and scores from the Vocabulary and Matrix Reasoning subtests were associated with graph theory measures at each proportion threshold level with Pearson pairwise correlations. Importantly, not all participants completed the WASI and thus correlations only included participants with complete observations. Outliers, defined as values above or below 3 standard deviations away from the mean, were removed before statistical analyses of graph theory measures and WASI subtests. All analyses were corrected for multiple comparisons with the false discovery rate (FDR) method (Benjamini and Hochberg, 1995).

Results

Demographic Information

Available demographic data for participants (CNTRL=36, ARND=9, FAS=13), including age at scan and the composition of the sample with respect to sex and condition, intelligence scores, and measures of motion are shown in Table 1. No significant differences between participant age were observed [$F(2,55)=0.74$, $p= 0.48$, $\eta^2_p=0.026$] nor were there differences in the representation of males and females in the sample following a chi square test [$X^2=0.78$, $p=0.48$].

Comparisons of Motion

Table 1 shows the results of a series of one-way ANOVAs with group (CNTRL, ARND, or FAS) as a main factor on measures of mean FD and FD in each translation and rotation direction. Significant omnibus tests were observed for FD, FD in the Y translation, and FD in the X rotation, but not in any of the other remaining FD directions.

Comparisons of the mean FD revealed a statistically significant omnibus effect of group [$F(2,57)=3.29$, $p=0.045$, $\eta^2_p=0.11$]. Follow-up post hoc tests revealed the mean framewise displacement of the ARND group ($\bar{x}=0.43$, $s=0.30$) was significantly higher when compared to that of the control group ($\bar{x}= 0.27$, $s=0.12$, $p=0.046$, $g=0.89$), but not higher than the FAS group ($\bar{x}=0.33$, $s=0.14$, $p=0.27$, $g=0.41$). Comparisons between the FAS and the CNTRL groups did not reveal a statistically significant difference ($p=0.27$, $g=0.46$).

One-way ANOVAs of the FD in the Y translation revealed a significant omnibus test of group [$F(2,55)=3.55$, $p=0.035$, $\eta^2_p=0.11$] and post hoc tests revealed the mean FD in the Y translation of the ARND group ($\bar{x}=0.17$, $s=0.11$) was significantly higher when compared to the CNTRL group ($\bar{x}=0.11$, $s=0.01$, $p=0.01$, $g=0.88$), but not the FAS group ($\bar{x}=0.11$, $s=0.01$, $p=0.054$, $g=0.77$). Controls did not differ significantly from the FAS group ($p=0.88$, $g=0.06$).

A one-way ANOVA of the mean FD in the X rotation also revealed a significant omnibus test of group [$F(2,55)=3.39$, $p=0.041$, $\eta^2_p=0.11$]. Follow-up post hoc tests revealed that the mean FD in the X rotation of the ARND group ($\bar{x}=0.06$, $s=0.03$) was significantly higher when compared to the CNTRL group ($\bar{x}=0.04$, $s=0.01$, $p=0.04$, $g=0.88$), but not the FAS group ($\bar{x}=0.04$, $s=0.01$, $p=0.23$, $g=0.42$). No significant differences were found between the FAS and CNTRL groups ($p=0.32$, $g=0.42$). Additional one-way ANOVAs on the remaining FD translation of rotation measures did not reveal any significant effects.

Graph Theory Measures

The results of separate group (CNTRL, ARND, FAS) by proportion threshold (0.1- 0.5) ANOVAs for each graph theory metric and between-group comparisons within each threshold level are displayed in Figure 1. Between-group comparisons within each threshold were conducted, even in the absence of a significant interaction because our aim was to investigate differences in network properties among PAE and CNTRL groups. For analyses of characteristic path length, one data point from a CNTRL participant at the 0.2 threshold was excluded as an outlier due to a value that exceed 3 standard deviations from the group mean. With the exception of the 0.2 threshold where the sample size was CNTRL=35, all remaining sample sizes for all other thresholds were CNTRL=36, ARND=9, and FAS=13 as no other outliers were detected for measures of modularity, the average clustering coefficient, nor global efficiency.

For measures of modularity (Figure 1A), no significant interaction between group and threshold was detected [$F(8,275)=1.37$, $p=0.21$, $\eta^2_p=0.40$]. In contrast, significant main effects of threshold [$F(4,275)=275.18$, $p<0.0001$, $\eta^2_p=0.8$] and group [$F(2, 275)=3.97$, $p<0.05$, $\eta^2_p=0.03$] were observed. The main effect of group was further investigated by tests of marginal means. However, results from these analyses did not reveal any significant differences between the ARND and CNTRL groups [$p=0.73$, $g=0.06$], FAS and CNTRL groups [$p=0.34$, $g=0.14$], nor between the ARND and FAS groups [$p=0.31$, $g=0.19$]. Between-group comparisons at each threshold level did not reveal any significant differences after FDR correction (all p's>0.10).

Analyses of the average clustering coefficient (Figure 1B) revealed no significant group by threshold interaction [$F(8,275)=0.33$, $p=0.95$, $\eta^2_p=0.01$], nor main effect of threshold [$F(4,275)=1.25$, $p=0.29$, $\eta^2_p=0.02$], but demonstrated a significant main effect of group [$F(8,275)=29.45$, $p<0.05$, $\eta^2_p=0.18$]. No significant between-group comparisons were observed within threshold 0.1 (all p's>0.16). In contrast, between-group comparisons revealed significant findings at thresholds 0.2 through 0.5. At threshold 0.2, CNTRL ($\bar{x}=0.25$, sd=0.03) < ARND [$\bar{x}=0.27$, sd=0.03, $p<0.05$, $g=0.78$], CNTRL > FAS [$\bar{x}=0.23$, sd=0.02, $p<0.05$, $g=0.66$], and ARND > FAS [$p<0.01$, $g=1.59$]. At threshold 0.3, CNTRL ($\bar{x}=0.25$, sd=0.03) < ARND [$\bar{x}=0.23$, sd=0.04, $p<0.05$, $g=0.74$], CNTRL > FAS [$\bar{x}=0.22$, sd=0.02, $p<0.05$, $g=.93$], and ARND > FAS [$p<0.01$, $g=1.51$]. Within threshold 0.4, CNTRL ($\bar{x}=0.24$, sd=0.02) < ARND [$\bar{x}=0.26$, sd=0.04, $p<0.05$, $g=0.80$], CNTRL > FAS [$\bar{x}=0.22$, sd=0.02, $p<0.05$, $g=.95$], and ARND > FAS [$p<0.01$, $g=1.55$]. At threshold 0.5, CNTRL ($\bar{x}=0.24$, sd=0.02) < ARND [$\bar{x}=0.26$, sd=0.04, $p<0.05$, $g=0.93$], CNTRL > FAS [$\bar{x}=0.22$, sd=0.01, $p<0.05$, $g=.94$], and ARND > FAS [$p<0.01$, $g=1.65$].

Analyses of characteristic path length (Figure 1C) revealed a significant group by threshold interaction [$F(8,274)=2.4$, $p=0.016$, $\eta^2_p=0.07$], main effect of threshold [$F(4,274)=163.49$, $p<0.05$, $\eta^2_p=0.71$], and main effect of group [$F(8,274)=10.83$, $p<0.05$, $\eta^2_p=0.07$]. No significant between-group comparisons were observed within threshold 0.1 (all p's>0.08). In contrast, between-group comparisons revealed a reoccurring pattern of lower mean characteristic path length in the ARND group when compared to the CNTRL group and lower mean characteristic path length in the ARND group relative to the FAS group at thresholds 0.2 through 0.5. For threshold 0.2, CNTRL ($\bar{x}=4.24$, sd=0.14) > ARND [$\bar{x}=4.03$, sd=0.22, $p<0.001$, $g=1.31$] and ARND < FAS [$\bar{x}=4.33$, sd=0.13, $p<0.0001$, $g=1.7$]. At threshold 0.3, CNTRL ($\bar{x}=3.80$, sd=0.13) > ARND [$\bar{x}=3.65$, sd=0.10, $p<0.001$, $g=1.21$], CNTRL < FAS

[$\bar{x}=3.89$, sd=0.08, $p<0.05$, g=0.71], and ARND < FAS [$p<0.0001$, g=2.5]. Within threshold 0.4, CNTRL ($\bar{x}=3.59$, sd=0.14) > ARND [$\bar{x}=3.42$, sd=0.14, $p<0.01$, g=1.16], CNTRL < FAS [$\bar{x}=3.69$, sd=0.09, $p<0.05$, g=0.77], and ARND < FAS [$p<0.0001$, g=2.32]. For threshold 0.5, CNTRL ($\bar{x}=3.51$, sd=0.15) > ARND [$\bar{x}=3.35$, sd=0.15, $p<0.001$, g=1.06], CNTRL < FAS [$\bar{x}=3.62$, sd=0.09, $p<0.05$, g=0.80], and ARND < FAS [$p<0.0001$, g=2.2].

For analyses of global efficiency (Figure 1D), a significant group by threshold interaction [$F(8,275)=4.06$, $p<0.0001$, $\eta^2_p=0.11$], main effect of threshold [$F(4,275)=988.04$, $p<0.05$, $\eta^2_p=0.935$], and main effect of group [$F(8,275)=12.612$, $p<0.05$, $\eta^2_p=0.08$] was observed. Between-group comparisons within threshold did not reveal any significant effects at thresholds 0.1 nor 0.2 (all *p*'s>0.21). However, between-group analyses revealed significant effects at thresholds 0.3 through 0.5. At threshold 0.3, CNTRL ($\bar{x}=0.31$, sd=0.01) < ARND [$\bar{x}=0.32$, sd=0.01, $p<0.05$, g=0.90], CNTRL > FAS [$\bar{x}=0.30$, sd=0.01, $p<0.05$, g=0.82], and ARND > FAS [$p<0.001$, g=2.18]. For threshold 0.4, CNTRL ($\bar{x}=0.32$, sd=0.02) < ARND [$\bar{x}=0.34$, sd=0.02, $p<0.01$, g=0.98], CNTRL > FAS [$\bar{x}=0.31$, sd=0.01, $p<0.05$, g=.82], and ARND > FAS [$p<0.001$, g=1.98]. At threshold 0.5, CNTRL ($\bar{x}=0.32$, sd=0.02) < ARND [$\bar{x}=0.34$, sd=0.02, $p<0.01$, g=1.05], CNTRL > FAS [$\bar{x}=0.31$, sd=0.01, $p<0.05$, g=.84], and ARND > FAS [$p<0.0001$, g=1.97].

In the present analyses, we adopted FDR correction for multiple comparisons because of the conservative nature of the Bonferroni approach, which reduces the Type I error rate, yet increases the Type II error rate. To communicate the outcome of these analyses under more conservative multiple correction criteria, we applied Bonferroni correction to the analyses and results are displayed in Supplementary Figure 3. Additionally, Supplementary Figure 4 displays the results of analyses between the CNTRL group and a combined FASD group that consisted of participants in the ARND and FAS groups and employed the FDR correction for multiple comparisons. The results of the combined alcohol exposed group did not reveal any statistically significant differences between the CNTRL and FASD groups in any of the network characteristics at any of the threshold levels examined.

Neuropsychological Measurements

WASI subtest t-scores and the estimated FS-IQ were compared using separate one-way ANOVAs utilizing group (CNTRL, FAS, or ARND) as the main factor. Not all participants returned for a post-scan neuropsychological assessment and subtest scores for some participants were missing. Thus, the following results were derived from available data. In addition, outliers, defined as any value above or below 3 standard deviations away from the mean within each group, resulted in the exclusion of one matrix reasoning subtest score from one participant in the CNTRL group. Sample sizes for analyses of FS-IQ were CNTRL=32, ARND=7, and FAS=12. Sample sizes for analyses of Vocabulary scores were CNTRL=32, ARND=7, and FAS=10. Sample sizes for analyses of Matrix Reasoning scores were CNTRL=31, ARND=7, and FAS=10.

The results of the one-way ANOVA conducted on measures for FS-IQ revealed a significant effect in the omnibus test [$F(2,48)=28$, $p<0.0001$, $\eta^2_p=0.54$]. Boxplots and results of between-group comparisons are displayed in Figure 2A and indicate the ARND ($\bar{x}=81.14$, $s=14.80$, $p<0.001$, $g=1.77$) and FAS groups ($\bar{x}=75.75$, $s=10.64$, $p<0.0001$, $g=2.33$) were significantly lower in FS-IQ estimates when compared to the CNTRL group ($\bar{x}=105.09$, $s=12.95$). However, a comparison of the FAS and ARND groups did not yield a statistically significant difference ($p=0.38$, $g=0.42$).

Results from a one-way ANOVA conducted on Vocabulary subtest scores are shown in Figure 2B. Analyses revealed a statistically significant effect in the omnibus test [$F(2,46)=39.27$, $p<0.0001$, $\eta^2_p=0.63$]. The ARND ($\bar{x}=30.71$, $s=10.48$, $p<0.0001$, $g=2.30$) and FAS ($\bar{x}=28.3$, $s=6.07$, $p<0.0001$, $g=2.79$) groups demonstrated significantly lower vocabulary scores when compared to the CNTRL group ($\bar{x}$=53.25, s=9.43). Similar to the measures of FS-IQ, no statistically significant differences were found between the FAS and ARND groups (p=0.59, g=0.28) in Vocabulary subtest scores.

Figure 2C displays results from a one-way ANOVA on Matrix reasoning measures which revealed a statistically significant effect in the omnibus test [F(2,45)=8.13, p<0.0001, $\eta^2_{p=}$.27]. Between-group comparisons revealed the FAS group ($\bar{x}$=41.3, s=10.06) had significantly lower Matrix reasoning scores when compared to the CNTRL group ($\bar{x}$=52.19, s=6.52, p<0.001, g=1.43). The FAS group also displayed significantly lower Matrix reasoning scores compared to those of the ARND group ($\bar{x}$=49.71, s=7.04, p<0.001, g=0.89). However, no significant difference between the CNTRL and ARND groups was observed (p=0.43, g=0.37).

Association of Neuropsychological Function to Graph Theory Measures

Available WASI subtest scores and IQ estimates were correlated to the average clustering coefficient, characteristic path length and global efficiency measures based on previous research indicating relationships between these graph theory metrics and measures of intelligence (Hilger et al., 2017, van den Heuvel et al., 2009, Kruschwitz et al., 2018) and are displayed in Figure 3. A full list of r-values, p-values, and confidence intervals are displayed in Supplementary Tables 2, 3, and 4.

In correlations between WASI scores and the average clustering coefficient (Figure 3A), only one correlation at the 0.1 threshold met the uncorrected α=0.05 level. This association was observed in the CNTRL group and was characterized by a negative association with matrix reasoning scores [r=-0.36, p=0.046]. With one exception at the 0.2 threshold for Vocabulary subtest scores, the FAS group displayed stronger correlations in the negative direction between WASI scores and the average clustering coefficient relative to the CNTRL group. However, these associations did not meet statistical significance. The ARND group primarily displayed weak associations between WASI scores and the average clustering coefficient at thresholds 0.2 – 0.5. Correlations between WASI scores and the average clustering coefficient in the ARND group did not meet statistical significance.

Four correlations between characteristic path length and Matrix Reasoning subtest scores (Figure 3B) met significance at uncorrected α=0.05 level for thresholds 0.1 [r=0.36, p=0.046], 0.3 [r=0.38, p=0.033], 0.4 [r=0.38, p=0.036], and 0.5 [r=0.38, p=0.041] for the CNTRL group only. The pattern of results is suggestive of positive associations between fluid intelligence and characteristic path length, but correlations did not survive FDR correction. No other correlations between WASI scores and characteristic path length for the ARND or FAS groups reached statistical significance despite modest correlations between characteristic path length and FS-IQ and characteristic path length and Matrix Reasoning subtest scores in the ARND group.

A total of four correlations between WASI scores and global efficiency met the uncorrected α=0.05 level and are displayed in Figure 3C. The CNTRL group displayed negative associations with Vocabulary subtest scores at the 0.1 [r=-0.39, p=-.026] threshold, and Matrix Reasoning subtest scores at the 0.3 [r=-0.37, p=0.038] and 0.4 [r=-0.36, p=0.045] thresholds. The FAS group exhibited one positive correlation between global efficiency and Matrix Reasoning subtest scores at the 0.1 threshold [r=0.67, p=0.033]. However, none of these correlations survived FDR correction.

Discussion

The present study compared global measures of functional network segregation and integration in a sample of adolescents and young adults diagnosed with FAS, ARND, and healthy controls at varying connection thresholds. In addition, measures of cognitive intelligence were compared between groups and correlated to network properties. Our analyses revealed differences in network characteristics and intelligence related to PAE, but significant relationships between graph metric and cognitive intelligence did not survive correction for multiple comparisons.

Network Characteristics

Global metrics of functional segregation included modularity and the average clustering coefficient. These network properties quantify the degree to which specialized information processing occurs within densely interconnected regions (Rubinov and Sporns, 2010). Measures of modularity did not significantly differ between groups. Global measures of network modularity have not been previously reported in studies of children, adolescents, nor adults with FASD. In contrast, multiple reports of disruptions in modularity have been documented in other pediatric neurodevelopmental disorders using functional connectivity measures derived from resting state fMRI data (Qian et al., 2019, Scariati et al., 2016).

The developmental trajectory of global modularity is characterized by an inverted U-shape (Gozdas et al., 2019) during adolescence and has been shown to be reduced in older compared to younger adult participants (Song et al., 2014). Moreover, research has documented sex-dependent differences in modularity in adolescents (males > females) (Gozdas et al., 2019). In light of these reports, our results for modularity may be related to the broad age range that spanned between 12-22 years. Additionally, it remains to be seen if modularity varies by sex in adolescents exposed to alcohol prenatally.

Measures of the average clustering coefficient between groups at thresholds 0.2 through 0.5 indicated significant reductions in the FAS group relative to the CNTRL and ARND groups that were accompanied by moderate and large effect sizes respectively. The ARND group also displayed significant increases in the average clustering coefficient relative to the CNTRL group along with large and moderate effect sizes respectively. Previous studies have documented, non-statistically significant increases in the average clustering coefficient in children and adolescents (Wozniak et al., 2017) with PAE and non-significant reductions in adolescents (Wozniak et al., 2013) and young children (Long et al., 2019) with PAE relative to controls.

Contrary to the findings of the developmental trajectory of global modularity measures (Gozdas et al., 2019), evidence suggests the average clustering coefficient remains relatively stable from childhood to adulthood (Fair et al., 2009) for whole brain connectivity and is not significantly different when compared between children and young adults in isolated networks of interest (Supekar et al., 2009). Given this previous research and the age-matched groups, we do not consider the network group differences in the average clustering coefficient to be a result of age. In the present study, measures of the average clustering coefficient across thresholds remained relatively stable.

Functional integration was assessed by comparing measures of characteristic path length and global efficiency which quantify the degree to which brain networks can combine specialized information from multiple regions (Rubinov and Sporns, 2010). Measures of characteristic path length consistently differed between the ARND and FAS groups and between the ARND and CNTRL groups at thresholds 0.2 – 0.5. Characteristic path length differed significantly between the FAS and CNTRL groups at threshold 0.3 – 0.5. In comparisons of characteristic path length between the FAS and CNTRL groups, effect sizes for thresholds 0.3 – 0.5 fell in the moderate to large range and may be suggestive of reduced network communication in the FAS group relative to the CNTRL group. Interestingly, characteristic path length was lower in the ARND group when compared to both the CNTRL and FAS groups at the aforementioned threshold levels. A lower characteristic path length can be interpreted as evidence of facilitated information transfer (Sporns, 2011) or higher connectivity because the measure is computed from the inverse of correlation values between the average component time courses and could be indicative of a compensatory mechanism. Previous studies examining children and adolescents with PAE have found statistically significant increases (Wozniak et al., 2013) and non-significant increases (Wozniak et al., 2017) in characteristic path length relative to controls. The two aforementioned studies both relied on the same regions of interest and binarized graphs to conduct network analysis, but differed in proportion threshold, sample age range, diagnostic system, and one study consisted of a large multi-site sample that used multiple MR scanner manufacturers and image acquisition sequences. However, a commonality amongst the Wozniak et al. studies is the direction of the effect with PAE youth displaying increases in path length relative to controls, which suggest impaired functional integration. The comparisons between the CNTRL and ARND groups in the present study oppose previous findings of increased characteristic path length associated with PAE. Furthermore, the ARND and FAS group displayed opposite effects when compared to the CNTRL group which could potentially explain null findings when comparing healthy controls to combined FASD groups. Similar to the average clustering coefficient, the characteristic path length remains relatively stable during development (Fair et al., 2009) and does not differ between children and young adults (Supekar et al., 2009) which suggests that our reported results and the differences between the two Wozniak et al. studies are unlikely to be explained by developmental effects related to age.

Measures of global efficiency were not significantly different between groups at thresholds 0.1 and 0.2. On the other hand, analyses revealed significant group differences at thresholds 0.3 – 0.5. These findings consistently indicated greater global efficiency in the ARND group when compared to the FAS group and CNTRL groups. Comparisons between the CNTRL and FAS groups indicated greater global efficiency in the CNTRL group for the aforementioned thresholds. Previous studies investigating global efficiency in individuals with FASD have documented both significant reductions in adolescents (Wozniak et al., 2013) and null findings in adolescents and young children (Long et al., 2019) with FASD relative to controls. As previously mentioned, these studies compared healthy controls to an aggregated alcohol-exposed group that may partially explain the disparate findings. Global efficiency increases from infancy to adolescence (Gozdas et al., 2019, Fan et al., 2020) and is reduced in older adults compared to younger adults (Achard and Bullmore, 2007) suggesting that global efficiency may display a protracted inverted U-shape trajectory across the life-span. No changes in global efficiency between children and young adults (Supekar et al., 2009) have also been documented, but this lack of consensus may be partially explained by the age ranges of the samples studied.

In the analyses of the average clustering coefficient, characteristic path length, and global efficiency, measures from the CNTRL group were flanked by those of the FAS and ARND groups at multiple thresholds. Prior studies of network connectivity in FASD have not examined differences between individuals with ARND and FAS sub-diagnoses as alcohol exposed participants are commonly placed into one group which may explain null results of network characteristics. To this point, we conducted a supplementary analysis comparing the CNTRL group to a combined FASD group that showed no differences in the four network characteristics examined. Additionally, the previous studies of global graph theory metrics in children and adolescents with FASD relied on different diagnostic systems that included the modified IOM criteria for the Wozniak et al., 2013 study and the Collaborative Initiative on Fetal Alcohol Spectrum Disorders (CIFASD) criteria for the Wozniak et al., 2017 study. In the Long et al., 2019 study, participants were too young to be diagnosed with a FASD and, as result, participants with confirmed PAE were compared to typically-developing controls. Thus, it cannot be ruled out that some of differences between the findings of the present and prior graph analyses are due to different diagnostic systems and this factor must be considered when making direct comparisons with prior or future studies with different classification systems.

PAE is associated with widespread abnormalities in brain structure and function. Among these, are changes to white matter integrity (Wozniak et al., 2011), cortical thickness (Yang et al., 2012), receptor expression (Galindo et al., 2004), neurotransmission (Varaschin et al., 2018), long-term potentiation (Sutherland et al., 1997), and structural synaptic plasticity (Rice et al., 2012), which could potentially explain changes in network properties, but are not accessible in the present investigation. Measures of path length and global efficiency have also been associated with genetic heritability (van den Heuvel et al., 2013, Fornito et al., 2011) and PAE is known to influence multiple epigenetic mechanisms that affect brain development (Lussier et al., 2017) which represent additional routes by which PAE can alter network characteristics. Furthermore, PAE can impact the development of other organ systems including the cardiovascular system (Cook et al., 2019) which can influence measures of functional connectivity (Carnevale et al., 2020) when assessed by fMRI.

The present findings suggest threshold-dependent patterns of abnormal network segregation and integration in individuals with FAS and ARND as measured by the average clustering coefficient, characteristic path length, and global efficiency. Measures of modularity were not significantly different between groups at any of the thresholds examined.

Neuropsychological Assessments

The current study also compared measures of cognitive intelligence assessed by the WASI two-subtest form with the aim of examining associations between network properties and measures of intellectual function. Results revealed that estimates of FS-IQ were significantly lower in the FAS and ARND groups when compared to the CNTRL group, but the FAS and ARND groups were not significantly different from each other. Similarly, comparisons of the Vocabulary subtest scores indicate both the FAS and ARND groups scored significantly lower when compared to the CNTRL group, but the FAS and ARND groups were not different from one another. For the Matrix Reasoning subtest, the FAS group scored significantly lower than the CNTRL group, but not lower than the ARND group. In addition, the ARND group did not score significantly differently than the CNTRL group in Matrix Reasoning.

Previous studies of alcohol exposed individuals have reported a mean IQ of 80 for non-dysmorphic participants (Mattson et al., 1997) and a mean IQ of 70 for those with FAS (Streissguth et al., 1991) and suggest that individuals with FAS are more severely impaired in intellectual functioning (Chasnoff et al., 2010). In the present study, the ARND group scored a mean IQ of 81 while the FAS group scored a mean IQ of 76 indicating partial concordance with previous reports. An investigation utilizing the 2nd edition of the four-subscale WASI also found reductions in FS-IQ, Verbal, and Matrix Reasoning performance in children with suspected FASD relative to neurotypically-developing controls (Popova et al., 2019). Collectively, our results coincide with previous research that suggest individuals with FAS are more severely impaired in measures of cognitive intelligence than individuals with ARND, although it is possible for individuals with ARND to be cognitively impaired at levels that are comparable to those with dysmorphic effects.

Correlations between behavior and network characteristics

The final aim of this study was to explore the relationship between measures of intelligence in each condition and measures of the average clustering coefficient, characteristic path length, and global efficiency. For each network metric, no significant correlations survived FDR correction at any of the thresholds examined (see Supplementary Tables 2, 3, and 4). These results partially align with a report that investigated the relationship between graph theory metrics and measures of crystallized and fluid intelligence utilizing multiple network definition schemes (including group ICA) and multiple connection densities in a large sample of nearly 1,000 healthy adult participants from the Human Connectome Project (Kruschwitz et al., 2018).

The authors reported no robust associations between global graph theory metrics and measures of cognitive intelligence. The present findings also mirror previous research suggesting that network characteristics are not strongly associated with intellectual functioning in adolescents with FASD (Wozniak et al., 2013).

Limitations and Future Directions

The interpretation of the results presented in this study require caution and consideration of several limitations. First, group sample sizes were unbalanced and small, especially for the FASD subgroups; ARND (n=9), FAS (n=13). Despite this, moderate and large effect sizes of between-group comparisons were observed in measures of the average clustering coefficient, characteristic path length, and global efficiency which indicate sample sizes were sufficient to detect effects. Additionally, the sample size of the present study was larger than prior studies of graph theory measures of network integration and segregation (van den Heuvel et al., 2009) and comparable to previous graph theory-based connectivity research in the FASD literature (Wozniak et al., 2013). It is also important to note that the age range of the sample was broad, spanning from 12 to 22 years. Although attempts were made to circumvent this problem via regressing out age on graph theory metrics, future investigations will benefit from narrower age ranges to rule out potential confounds due to maturational effects.

Second, not all participants completed neuropsychological assessments that led to sample size reductions for correlating network properties with cognitive intelligence. Relatedly, the two-subtest form of the WASI utilized in this study, is a coarse measure of intelligence in comparison to the four-subtest measure and other available instruments. Moreover, it remains to be seen if other neuropsychological assessments or measures of cognitive processes, such as attention, working memory, or response inhibition are related to network analysis measures.

Third, as previously noted, the ARND group in this study demonstrated higher levels of head motion when compared to the CNTRL group. Head motion is undesirable in fMRI studies as it can contaminate the BOLD signal with artefactual features leading to changes in functional connectivity that could be mistaken for neuronal effects (Van Dijk et al., 2012, Satterthwaite et al., 2012, Power et al., 2012). Thus, it cannot be ruled out that the pattern of results for the ARND group were related to higher levels of head motion. On the other hand, although not statistically different, the FAS group also had higher levels of head motion compared to the CNTRL group, yet the pattern of results observed for the FAS group were primarily in the opposite direction of the ARND group when compared to the CNTRL group and future research in this area will be especially important to confirm sub-diagnostic dependent changes in functional network connectivity associated with PAE.

Fourth, although our approach consisted of a small number of ICs as nodes in comparison to graph theory studies that utilized network definition schemes consisting of up to 200 regions of interest, the number of components used in the present report is consistent with prior studies relying on gICA of fMRI data (Allen et al., 2011, Vergara et al., 2018). In the present study, some ICs consisted of multiple brain regions and thus some nodes represent networks and interpretation of the reported graph theory metrics must take this into account when comparing to other studies.

Finally, the connectivity measures between ICs are averaged across the fMRI scan session and do not capture potential changes in network configurations (Chang and Glover, 2010) that may occur during the scanning period. Additional research employing dynamic functional network connectivity approaches may address this limitation and prove informative for the field (Yu et al., 2018).

Conclusions

FASD remains a significant public health concern with far reaching societal implications and economic costs. The current study adds to a growing body of evidence of the potential consequences of PAE on brain network properties and their relationship to neuropsychological function. We demonstrated that PAE is most strongly linked to changes in network segregation as assessed by the average clustering coefficient and in network integration as assessed by the characteristic path length and global efficiency. Interestingly, the ARND and FAS groups demonstrated opposing results when compared to the CNTRL group. Additionally, measures of segregation and integration were not strongly related to measures of cognitive intelligence in participants exposed to alcohol prenatally nor in healthy controls.

Acknowledgements: The authors would like to thank Dr. John F.L. Pinner for assistance in friendly review of this manuscript.

References

ACHARD, S. & BULLMORE, E. T. 2007. Efficiency and cost of economical brain functional networks. *Plos Computational Biology,* 3**,** 174-183.

ALLEN, E. A., ERHARDT, E. B., DAMARAJU, E., GRUNER, W., SEGALL, J. M., SILVA, R. F., HAVLICEK, M., RACHAKONDA, S., FRIES, J., KALYANAM, R., MICHAEL, A. M., CAPRIHAN, A., TURNER, J. A., EICHELE, T., ADELSHEIM, S., BRYAN, A. D., BUSTILLO, J., CLARK, V. P., FELDSTEIN EWING, S. W., FILBEY, F., FORD, C. C., HUTCHISON, K., JUNG, R. E., KIEHL, K. A., KODITUWAKKU, P., KOMESU, Y. M., MAYER, A. R., PEARLSON, G. D., PHILLIPS, J. P., SADEK, J. R., STEVENS, M., TEUSCHER, U., THOMA, R. J. & CALHOUN, V. D. 2011. A baseline for the multivariate comparison of resting-state networks. *Front Syst Neurosci,* 5**,** 2.

ASTLEY, S. J., AYLWARD, E. H., OLSON, H. C., KERNS, K., BROOKS, A., COGGINS, T. E., DAVIES, J., DORN, S., GENDLER, B., JIRIKOWIC, T., KRAEGEL, P., MARAVILLA, K. & RICHARDS, T. 2009. Functional magnetic resonance imaging outcomes from a comprehensive magnetic resonance study of children with fetal alcohol spectrum disorders. *J Neurodev Disord,* 1**,** 61-80.

BENJAMINI, Y. & HOCHBERG, Y. 1995. Controlling the False Discovery Rate - a Practical and Powerful Approach to Multiple Testing. *Journal of the Royal Statistical Society Series B-Statistical Methodology,* 57**,** 289-300.

BULLMORE, E. T. & BASSETT, D. S. 2011. Brain graphs: graphical models of the human brain connectome. *Annu Rev Clin Psychol,* 7**,** 113-40.

CARNEVALE, L., MAFFEI, A., LANDOLFI, A., GRILLEA, G., CARNEVALE, D. & LEMBO, G. 2020. Brain Functional Magnetic Resonance Imaging Highlights Altered Connections and Functional Networks in Patients With Hypertension. *Hypertension,* 76**,** 1480-1490.

CHANG, C. & GLOVER, G. H. 2010. Time-frequency dynamics of resting-state brain connectivity measured with fMRI. *Neuroimage,* 50**,** 81-98.

CHASNOFF, I. J., WELLS, A. M., TELFORD, E., SCHMIDT, C. & MESSER, G. 2010. Neurodevelopmental functioning in children with FAS, pFAS, and ARND. *J Dev Behav Pediatr,* 31**,** 192-201.

CHEN, X., COLES, C. D., LYNCH, M. E. & HU, X. 2012. Understanding specific effects of prenatal alcohol exposure on brain structure in young adults. *Hum Brain Mapp,* 33**,** 1663-76.

COFFMAN, B. A., KODITUWAKKU, P., KODITUWAKKU, E. L., ROMERO, L., SHARADAMMA, N. M., STONE, D. & STEPHEN, J. M. 2013. Primary visual response (M100) delays in adolescents with FASD as measured with MEG. *Hum Brain Mapp,* 34**,** 2852-62.

COLES, C. D., GOLDSTEIN, F. C., LYNCH, M. E., CHEN, X. C., KABLE, J. A., JOHNSON, K. C. & HU, X. P. 2011. Memory and brain volume in adults prenatally exposed to alcohol. *Brain and Cognition,* 75**,** 67-77.

COOK, J. C., LYNCH, M. E. & COLES, C. D. 2019. Association Analysis: Fetal Alcohol Spectrum Disorder and Hypertension Status in Children and Adolescents. *Alcohol Clin Exp Res,* 43**,** 1727-1733.

COX, R. W. 1996. AFNI: software for analysis and visualization of functional magnetic resonance neuroimages. *Comput Biomed Res,* 29**,** 162-73.

FAIR, D. A., COHEN, A. L., POWER, J. D., DOSENBACH, N. U., CHURCH, J. A., MIEZIN, F. M., SCHLAGGAR, B. L. & PETERSEN, S. E. 2009. Functional brain networks develop from a "local to distributed" organization. *PLoS Comput Biol,* 5**,** e1000381.

FAN, F., LIAO, X., LEI, T., ZHAO, T., XIA, M., MEN, W., WANG, Y., HU, M., LIU, J., QIN, S., TAN, S., GAO, J. H., DONG, Q., TAO, S. & HE, Y. 2020. Development of the Default-

Mode Network during Childhood and Adolescence: A Longitudinal Resting-State fMRI Study. *Neuroimage***,** 117581.

FAN, J., TAYLOR, P. A., JACOBSON, S. W., MOLTENO, C. D., GOHEL, S., BISWAL, B. B., JACOBSON, J. L. & MEINTJES, E. M. 2017. Localized reductions in resting-state functional connectivity in children with prenatal alcohol exposure. *Hum Brain Mapp,* 38**,** 5217-5233.

FORNITO, A., ZALESKY, A., BASSETT, D. S., MEUNIER, D., ELLISON-WRIGHT, I., YUCEL, M., WOOD, S. J., SHAW, K., O'CONNOR, J., NERTNEY, D., MOWRY, B. J., PANTELIS, C. & BULLMORE, E. T. 2011. Genetic influences on cost-efficient organization of human cortical functional networks. *J Neurosci,* 31**,** 3261-70.

FORNITO, A., ZALESKY, A. & BULLMORE, E. T. 2016. *Fundamentals of brain network analysis*.

FRISTON, K. J., HOLMES, A. P., WORSLEY, K. J., POLINE, J. P., FRITH, C. D. & FRACKOWIAK, R. S. J. 1994. Statistical parametric maps in functional imaging: A general linear approach. *Human Brain Mapping,* 2**,** 189-210.

FRYER, S. L., TAPERT, S. F., MATTSON, S. N., PAULUS, M. P., SPADONI, A. D. & RILEY, E. P. 2007. Prenatal alcohol exposure affects frontal-striatal BOLD response during inhibitory control. *Alcohol Clin Exp Res,* 31**,** 1415-24.

GALINDO, R., FRAUSTO, S., WOLFF, C., CALDWELL, K. K., PERRONE-BIZZOZERO, N. I. & SAVAGE, D. D. 2004. Prenatal ethanol exposure reduces mGluR(5) receptor number and function in the dentate gyrus of adult offspring. *Alcoholism-Clinical and Experimental Research,* 28**,** 1587-1597.

GOZDAS, E., HOLLAND, S. K., ALTAYE, M. & CONSORTIUM, C. A. 2019. Developmental changes in functional brain networks from birth through adolescence. *Hum Brain Mapp,* 40**,** 1434-1444.

HILGER, K., EKMAN, M., FIEBACH, C. J. & BASTEN, U. 2017. Intelligence is associated with the modular structure of intrinsic brain networks. *Sci Rep,* 7**,** 16088.

HOYME, H. E., MAY, P. A., KALBERG, W. O., KODITUWAKKU, P., GOSSAGE, J. P., TRUJILLO, P. M., BUCKLEY, D. G., MILLER, J. H., ARAGON, A. S., KHAOLE, N., VILJOEN, D. L., JONES, K. L. & ROBINSON, L. K. 2005. A practical clinical approach to diagnosis of fetal alcohol spectrum disorders: clarification of the 1996 institute of medicine criteria. *Pediatrics,* 115**,** 39-47.

KAZEMINEJAD, A. & SOTERO, R. C. 2020. The Importance of Anti-correlations in Graph Theory Based Classification of Autism Spectrum Disorder. *Front Neurosci,* 14**,** 676.

KONRAD, K., NEUFANG, S., THIEL, C. M., SPECHT, K., HANISCH, C., FAN, J., HERPERTZ-DAHLMANN, B. & FINK, G. R. 2005. Development of attentional networks: an fMRI study with children and adults. *Neuroimage,* 28**,** 429-39.

KRUSCHWITZ, J. D., WALLER, L., DAEDELOW, L. S., WALTER, H. & VEER, I. M. 2018. General, crystallized and fluid intelligence are not associated with functional global network efficiency: A replication study with the human connectome project 1200 data set. *Neuroimage,* 171**,** 323-331.

LATORA, V. & MARCHIORI, M. 2001. Efficient behavior of small-world networks. *Physical Review Letters,* 87.

LITTLE, G., REYNOLDS, J. & BEAULIEU, C. 2018. Altered Functional Connectivity Observed at Rest in Children and Adolescents Prenatally Exposed to Alcohol. *Brain Connect,* 8**,** 503-515.

LONG, X., KAR, P., GIBBARD, B., TORTORELLI, C. & LEBEL, C. 2019. The brain's functional connectome in young children with prenatal alcohol exposure. *Neuroimage Clin,* 24**,** 102082.

LONG, X., LITTLE, G., BEAULIEU, C. & LEBEL, C. 2018. Sensorimotor network alterations in children and youth with prenatal alcohol exposure. *Hum Brain Mapp,* 39**,** 2258-2268.

LONG, X., LITTLE, G., TREIT, S., BEAULIEU, C., GONG, G. & LEBEL, C. 2020. Altered brain white matter connectome in children and adolescents with prenatal alcohol exposure. *Brain Struct Funct,* 225, 1123-1133.

LUSSIER, A. A., WEINBERG, J. & KOBOR, M. S. 2017. Epigenetics studies of fetal alcohol spectrum disorder: where are we now? *Epigenomics,* 9, 291-311.

MA, X., COLES, C. D., LYNCH, M. E., LACONTE, S. M., ZURKIYA, O., WANG, D. & HU, X. 2005. Evaluation of corpus callosum anisotropy in young adults with fetal alcohol syndrome according to diffusion tensor imaging. *Alcohol Clin Exp Res,* 29, 1214-22.

MALISZA, K. L., ALLMAN, A. A., SHILOFF, D., JAKOBSON, L., LONGSTAFFE, S. & CHUDLEY, A. E. 2005. Evaluation of spatial working memory function in children and adults with fetal alcohol spectrum disorders: a functional magnetic resonance imaging study. *Pediatr Res,* 58, 1150-7.

MATTSON, S. N., RILEY, E. P., GRAMLING, L., DELIS, D. C. & JONES, K. L. 1997. Heavy prenatal alcohol exposure with or without physical features of fetal alcohol syndrome leads to IQ deficits. *J Pediatr,* 131, 718-21.

MAY, P. A., BAETE, A., RUSSO, J., ELLIOTT, A. J., BLANKENSHIP, J., KALBERG, W. O., BUCKLEY, D., BROOKS, M., HASKEN, J., ABDUL-RAHMAN, O., ADAM, M. P., ROBINSON, L. K., MANNING, M. & HOYME, H. E. 2014. Prevalence and characteristics of fetal alcohol spectrum disorders. *Pediatrics,* 134, 855-66.

MAY, P. A., CHAMBERS, C. D., KALBERG, W. O., ZELLNER, J., FELDMAN, H., BUCKLEY, D., KOPALD, D., HASKEN, J. M., XU, R., HONERKAMP-SMITH, G., TARAS, H., MANNING, M. A., ROBINSON, L. K., ADAM, M. P., ABDUL-RAHMAN, O., VAUX, K., JEWETT, T., ELLIOTT, A. J., KABLE, J. A., AKSHOOMOFF, N., FALK, D., ARROYO, J. A., HERELD, D., RILEY, E. P., CHARNESS, M. E., COLES, C. D., WARREN, K. R., JONES, K. L. & HOYME, H. E. 2018. Prevalence of Fetal Alcohol Spectrum Disorders in 4 US Communities. *JAMA,* 319, 474-482.

MEINTJES, E. M., JACOBSON, J. L., MOLTENO, C. D., GATENBY, J. C., WARTON, C., CANNISTRACI, C. J., HOYME, H. E., ROBINSON, L. K., KHAOLE, N., GORE, J. C. & JACOBSON, S. W. 2010. An FMRI study of number processing in children with fetal alcohol syndrome. *Alcohol Clin Exp Res,* 34, 1450-64.

NEWMAN, M. E. J. 2006. Modularity and community structure in networks. *Proceedings of the National Academy of Sciences of the United States of America,* 103, 8577-8582.

ONNELA, J. P., SARAMAKI, J., KERTESZ, J. & KASKI, K. 2005. Intensity and coherence of motifs in weighted complex networks. *Phys Rev E Stat Nonlin Soft Matter Phys,* 71, 065103.

POPOVA, S., LANGE, S., POZNYAK, V., CHUDLEY, A. E., SHIELD, K. D., REYNOLDS, J. N., MURRAY, M. & REHM, J. 2019. Population-based prevalence of fetal alcohol spectrum disorder in Canada. *BMC Public Health,* 19, 845.

POWER, J. D., BARNES, K. A., SNYDER, A. Z., SCHLAGGAR, B. L. & PETERSEN, S. E. 2012. Spurious but systematic correlations in functional connectivity MRI networks arise from subject motion. *Neuroimage,* 59, 2142-54.

QIAN, X., CASTELLANOS, F. X., UDDIN, L. Q., LOO, B. R. Y., LIU, S., KOH, H. L., POH, X. W. W., FUNG, D., GUAN, C., LEE, T. S., LIM, C. G. & ZHOU, J. 2019. Large-scale brain functional network topology disruptions underlie symptom heterogeneity in children with attention-deficit/hyperactivity disorder. *Neuroimage Clin,* 21, 101600.

R DEVELOPMENT CORE TEAM 2020. R: A language and environment for statistical computing. Vienna, Austria: R Foundation for Statistical Computing.

RICE, J. P., SUGGS, L. E., LUSK, A. V., PARKER, M. O., CANDELARIA-COOK, F. T., AKERS, K. G., SAVAGE, D. D. & HAMILTON, D. A. 2012. Effects of exposure to moderate levels of ethanol during prenatal brain development on dendritic length, branching, and spine density in the nucleus accumbens and dorsal striatum of adult rats. *Alcohol,* 46, 577-84.

RILEY, E. P., MATTSON, S. N., SOWELL, E. R., JERNIGAN, T. L., SOBEL, D. F. & JONES, K. L. 1995. Abnormalities of the corpus callosum in children prenatally exposed to alcohol. *Alcohol Clin Exp Res,* 19, 1198-202.

RUBINOV, M. & SPORNS, O. 2010. Complex network measures of brain connectivity: uses and interpretations. *Neuroimage,* 52, 1059-69.

SANTHANAM, P., COLES, C. D., LI, Z., LI, L., LYNCH, M. E. & HU, X. 2011. Default mode network dysfunction in adults with prenatal alcohol exposure. *Psychiatry Res,* 194, 354-62.

SANTHANAM, P., LI, Z., HU, X., LYNCH, M. E. & COLES, C. D. 2009. Effects of prenatal alcohol exposure on brain activation during an arithmetic task: an fMRI study. *Alcohol Clin Exp Res,* 33, 1901-8.

SATTERTHWAITE, T. D., WOLF, D. H., LOUGHEAD, J., RUPAREL, K., ELLIOTT, M. A., HAKONARSON, H., GUR, R. C. & GUR, R. E. 2012. Impact of in-scanner head motion on multiple measures of functional connectivity: relevance for studies of neurodevelopment in youth. *Neuroimage,* 60, 623-32.

SCARIATI, E., SCHAER, M., KARAHANOGLU, I., SCHNEIDER, M., RICHIARDI, J., DEBBANE, M., VAN DE VILLE, D. & ELIEZ, S. 2016. Large-scale functional network reorganization in 22q11.2 deletion syndrome revealed by modularity analysis. *Cortex,* 82, 86-99.

SOKOL, R. J., DELANEY-BLACK, V. & NORDSTROM, B. 2003. Fetal alcohol spectrum disorder. *JAMA,* 290, 2996-9.

SONG, J., BIRN, R. M., BOLY, M., MEIER, T. B., NAIR, V. A., MEYERAND, M. E. & PRABHAKARAN, V. 2014. Age-related reorganizational changes in modularity and functional connectivity of human brain networks. *Brain Connect,* 4, 662-76.

SPORNS, O. 2011. *Networks of the brain,* Cambridge, Mass., MIT Press.

STREISSGUTH, A. P., AASE, J. M., CLARREN, S. K., RANDELS, S. P., LADUE, R. A. & SMITH, D. F. 1991. Fetal alcohol syndrome in adolescents and adults. *JAMA,* 265, 1961-7.

SUPEKAR, K., MUSEN, M. & MENON, V. 2009. Development of large-scale functional brain networks in children. *PLoS Biol,* 7, e1000157.

SUTHERLAND, R. J., MCDONALD, R. J. & SAVAGE, D. D. 1997. Prenatal exposure to moderate levels of ethanol can have long-lasting effects on hippocampal synaptic plasticity in adult offspring. *Hippocampus,* 7, 232-8.

TESCHE, C. D., KODITUWAKKU, P. W., GARCIA, C. M. & HOUCK, J. M. 2015. Sex-related differences in auditory processing in adolescents with fetal alcohol spectrum disorder: A magnetoencephalographic study. *Neuroimage Clin,* 7, 571-87.

VAKHTIN, A. A., KODITUWAKKU, P. W., GARCIA, C. M. & TESCHE, C. D. 2015. Aberrant development of post-movement beta rebound in adolescents and young adults with fetal alcohol spectrum disorders. *Neuroimage Clin,* 9, 392-400.

VAN DEN HEUVEL, M. P., STAM, C. J., KAHN, R. S. & POL, H. E. H. 2009. Efficiency of Functional Brain Networks and Intellectual Performance. *Journal of Neuroscience,* 29, 7619-7624.

VAN DEN HEUVEL, M. P., VAN SOELEN, I. L., STAM, C. J., KAHN, R. S., BOOMSMA, D. I. & HULSHOFF POL, H. E. 2013. Genetic control of functional brain network efficiency in children. *Eur Neuropsychopharmacol,* 23, 19-23.

VAN DIJK, K. R., SABUNCU, M. R. & BUCKNER, R. L. 2012. The influence of head motion on intrinsic functional connectivity MRI. *Neuroimage,* 59, 431-8.

VARASCHIN, R. K., ALLEN, N. A., ROSENBERG, M. J., VALENZUELA, C. F. & SAVAGE, D. D. 2018. Prenatal Alcohol Exposure Increases Histamine H3 Receptor-Mediated Inhibition of Glutamatergic Neurotransmission in Rat Dentate Gyrus. *Alcohol Clin Exp Res,* 42, 295-305.

VERGARA, V. M., MAYER, A. R., KIEHL, K. A. & CALHOUN, V. D. 2018. Dynamic functional network connectivity discriminates mild traumatic brain injury through machine learning. *Neuroimage Clin,* 19**,** 30-37.

WATTS, D. J. & STROGATZ, S. H. 1998. Collective dynamics of 'small-world' networks. *Nature,* 393**,** 440-442.

WECHSLER, D. 2009. Wechsler Abbreviated Scale of Intelligence. San Antonio, TX: Psychological Corporation.

WOZNIAK, J. R., MUELLER, B. A., BELL, C. J., MUETZEL, R. L., HOECKER, H. L., BOYS, C. J. & LIM, K. O. 2013. Global functional connectivity abnormalities in children with fetal alcohol spectrum disorders. *Alcohol Clin Exp Res,* 37**,** 748-56.

WOZNIAK, J. R., MUELLER, B. A., MATTSON, S. N., COLES, C. D., KABLE, J. A., JONES, K. L., BOYS, C. J., LIM, K. O., RILEY, E. P., SOWELL, E. R. & CIFASD 2017. Functional connectivity abnormalities and associated cognitive deficits in fetal alcohol Spectrum disorders (FASD). *Brain Imaging Behav,* 11**,** 1432-1445.

WOZNIAK, J. R., MUELLER, B. A., MUETZEL, R. L., BELL, C. J., HOECKER, H. L., NELSON, M. L., CHANG, P. N. & LIM, K. O. 2011. Inter-hemispheric functional connectivity disruption in children with prenatal alcohol exposure. *Alcohol Clin Exp Res,* 35**,** 849-61.

WOZNIAK, J. R., MUETZEL, R. L., MUELLER, B. A., MCGEE, C. L., FREERKS, M. A., WARD, E. E., NELSON, M. L., CHANG, P. N. & LIM, K. O. 2009. Microstructural corpus callosum anomalies in children with prenatal alcohol exposure: an extension of previous diffusion tensor imaging findings. *Alcohol Clin Exp Res,* 33**,** 1825-35.

YANG, Y., ROUSSOTTE, F., KAN, E., SULIK, K. K., MATTSON, S. N., RILEY, E. P., JONES, K. L., ADNAMS, C. M., MAY, P. A., O'CONNOR, M. J., NARR, K. L. & SOWELL, E. R. 2012. Abnormal cortical thickness alterations in fetal alcohol spectrum disorders and their relationships with facial dysmorphology. *Cereb Cortex,* 22**,** 1170-9.

YU, Q., DU, Y., CHEN, J., SUI, J., ADALĒ, T., PEARLSON, G. D. & CALHOUN, V. D. 2018. Application of Graph Theory to Assess Static and Dynamic Brain Connectivity: Approaches for Building Brain Graphs. *Proceedings of the IEEE,* 106**,** 886-906.

ZHOU, D., LEBEL, C., LEPAGE, C., RASMUSSEN, C., EVANS, A., WYPER, K., PEI, J., ANDREW, G., MASSEY, A., MASSEY, D. & BEAULIEU, C. 2011. Developmental cortical thinning in fetal alcohol spectrum disorders. *Neuroimage,* 58**,** 16-25.

Figure Captions

Figure 1 Boxplots and results of between-group comparisons of graph theory metrics within threshold. Solid horizontal lines within each box represent the median, while dotted lines represent the mean. Panel A) modularity; B) clustering coefficient, C) characteristic path length, D) global efficiency. CNTRL, controls; ARND, alcohol neurodevelopmental disorder, FAS, fetal alcohol syndrome. ****, p<0.0001; ***, p<0.001; **, p<0.01; *, p<0.05. All p values are corrected by FDR method. For analyses of characteristic path length, one data point from a CNTRL participant at the 0.2 threshold was excluded as an outlier resulting in a sample size of 35. All other remaining sample sizes were CNTRL=36, ARND=9, and FAS=13.

Figure 2 Boxplots and results of between-group comparisons of WASI full-scale IQ and subtest scores. Solid horizontal lines within each box represent the median, while dotted lines represent the mean. Panel A) mean WASI FS-IQ estimate, B) mean Vocabulary subtests scores, C) mean Matrix Reasoning scores. CNTRL, controls; ARND, alcohol related neurodevelopmental disorder; FAS, fetal alcohol syndrome; WASI, Wechsler's abbreviated scale of intelligence. ****, p<0.0001; ***, p<0.001; **, p<0.01; *, p<0.05. All p values are corrected by FDR method. Sample sizes for FS-IQ estimates were CNTRL=32, ARND=7, and FAS=12. Sample sizes for Vocabulary scores were CNTRL=32, ARND=7, and FAS=10. Sample sizes for Matrix Reasoning scores were CNTRL=31, ARND=7, and FAS=10.

Figure 3 Correlations between graph theory metrics and WASI FS-IQ and subtest scores at multiple threshold levels. Panel A), WASI – average clustering coefficient correlations, B) WASI – characteristic path length correlations, C) WASI – global efficiency correlations. CNTRL, controls; ARND, alcohol related neurodevelopmental disorder; FAS, fetal alcohol syndrome;

WASI, Wechsler's abbreviated scale of intelligence. Individual correlations were tested against the null hypothesis r=0 with a two tailed one sample t-test. *, $p<0.05$ (uncorrected). Sample sizes for FS-IQ estimates were CNTRL=32, ARND=7, and FAS=12. Sample sizes for Vocabulary scores were CNTRL=32, ARND=7, and FAS=10. Sample sizes for Matrix Reasoning scores were CNTRL=31, ARND=7, and FAS=10.

Table 1 – Demographic Characteristics and Summary Statistics of Measures of Motion and Intelligence. Values expressed as the mean (standard deviation). The displayed *p*-values stem from an omnibus test of a one-way ANOVA for continuous variables (age, FS-IQ, Vocabulary, and Matrix Reasoning subtest scores, and motion characteristics) and chi-square test for categorical variables (sex). FD; X, Y, Z translations; Rot X, Y, Z, rotations. s, standard deviation. † Two participants each from the ARND and FAS groups did not complete neuropsychological assessments. A set of Vocabulary and Matrix subtest scores from the same CNTRL participant were identified as outliers and excluded from analyses.

	level	CNTRL	ARND	FAS	p
Number of scans analyzed		36	9	13	
Age_Years (mean (sd))		16.33 (2.49)	17.20 (3.04)	15.78 (2.96)	0.482
Sex (number(%))	M	20 (55.6)	5 (55.6)	9 (69.2)	0.678
	F	16 (44.4)	4 (44.4)	4 (30.8)	
IQ (mean (sd))		105.09 (12.95)	81.14 (14.80)	75.75 (10.64)	<0.0001
Number of FS-IQ datapoints †		32	7	12	
Vocabulary (mean (sd))		52.54 (8.69)	30.71 (10.48)	28.30 (6.07)	<0.0001
Number of Vocabulary datapoints †		31	7	10	
Matrix Reasoning (mean (sd))		50.81 (7.73)	49.71 (7.04)	41.30 (10.06)	0.009
Number of Matrix datapoints †		31	7	10	
Mean_FWD (mean (sd))		0.27 (0.12)	0.43 (0.30)	0.33 (0.14)	0.045
Mean_FWD_X (mean (sd))		0.02 (0.01)	0.04 (0.03)	0.03 (0.03)	0.102
Mean_FWD_Y (mean (sd))		0.10 (0.06)	0.17 (0.11)	0.11 (0.04)	0.035
Mean_FWD_Z (mean (sd))		0.07 (0.04)	0.10 (0.09)	0.09 (0.05)	0.119
Mean_FWD_Rot_X (mean (sd))		0.04 (0.01)	0.06 (0.03)	0.04 (0.01)	0.041
Mean_FWD_Rot_Y (mean (sd))		0.03 (0.01)	0.04 (0.03)	0.04 (0.03)	0.099
Mean_FWD_Rot_Z (mean (sd))		0.02 (0.01)	0.02 (0.02)	0.02 (0.02)	0.201

Figure 1 Boxplots and results of between-group comparisons of graph theory metrics within threshold. Solid horizontal lines within each box represent the median, while dotted lines represent the mean. Panel A) modularity; B) clustering coefficient, C) characteristic path length, D) global efficiency. CNTRL, controls; ARND, alcohol neurodevelopmental disorder, FAS, fetal alcohol syndrome. ****, p<0.0001; ***, p<0.001; **, p<0.01; *, p<0.05. All p values are corrected by FDR method. For analyses of characteristic path length, one data point from a CNTRL participant at the 0.2 threshold was excluded as an outlier resulting in a sample size of 35. All other remaining sample sizes were CNTRL=36, ARND=9, and FAS=13.

Figure 2 Boxplots and results of between-group comparisons of WASI full-scale IQ and subtest scores. Solid horizontal lines within each box represent the median, while dotted lines represent the mean. Panel A) mean WASI FS-IQ estimate, B) mean Vocabulary subtests scores, C) mean Matrix Reasoning scores. CNTRL, controls; ARND, alcohol related neurodevelopmental disorder; FAS, fetal alcohol syndrome; WASI, Weschler's abbreviated scale of intelligence. ****, p<0.0001; ***, p<0.001; **, p<0.01; *, p<0.05. All p values are corrected by FDR method. Sample sizes for FS-IQ estimates were CNTRL=32, ARND=7, and FAS=12. Sample sizes for Vocab scores were CNTRL=32, ARND=7, and FAS=10. Sample sizes for Matrix Reasoning scores were CNTRL=31, ARND=7, and FAS=10.

Figure 3 Correlations between graph theory metrics and WASI FS-IQ and subtest scores at multiple threshold levels. Panel A), WASI – average clustering coefficient correlations, B) WASI – characteristic path length correlations, C) WASI – global efficiency correlations. CNTRL, controls; ARND, alcohol related neurodevelopmental disorder; FAS, fetal alcohol syndrome; WASI, Weschler's abbreviated scale of intelligence. Individual correlations were tested against the null hypothesis $r=0$ with a two tailed one sample t-test. *, $p<0.05$ (uncorrected). Sample sizes for FS-IQ estimates were CNTRL=32, ARND=7, and FAS=12. Sample sizes for Vocab scores were CNTRL=32, ARND=7, and FAS=10. Sample sizes for Matrix Reasoning scores were CNTRL=31, ARND=7, and FAS=10.

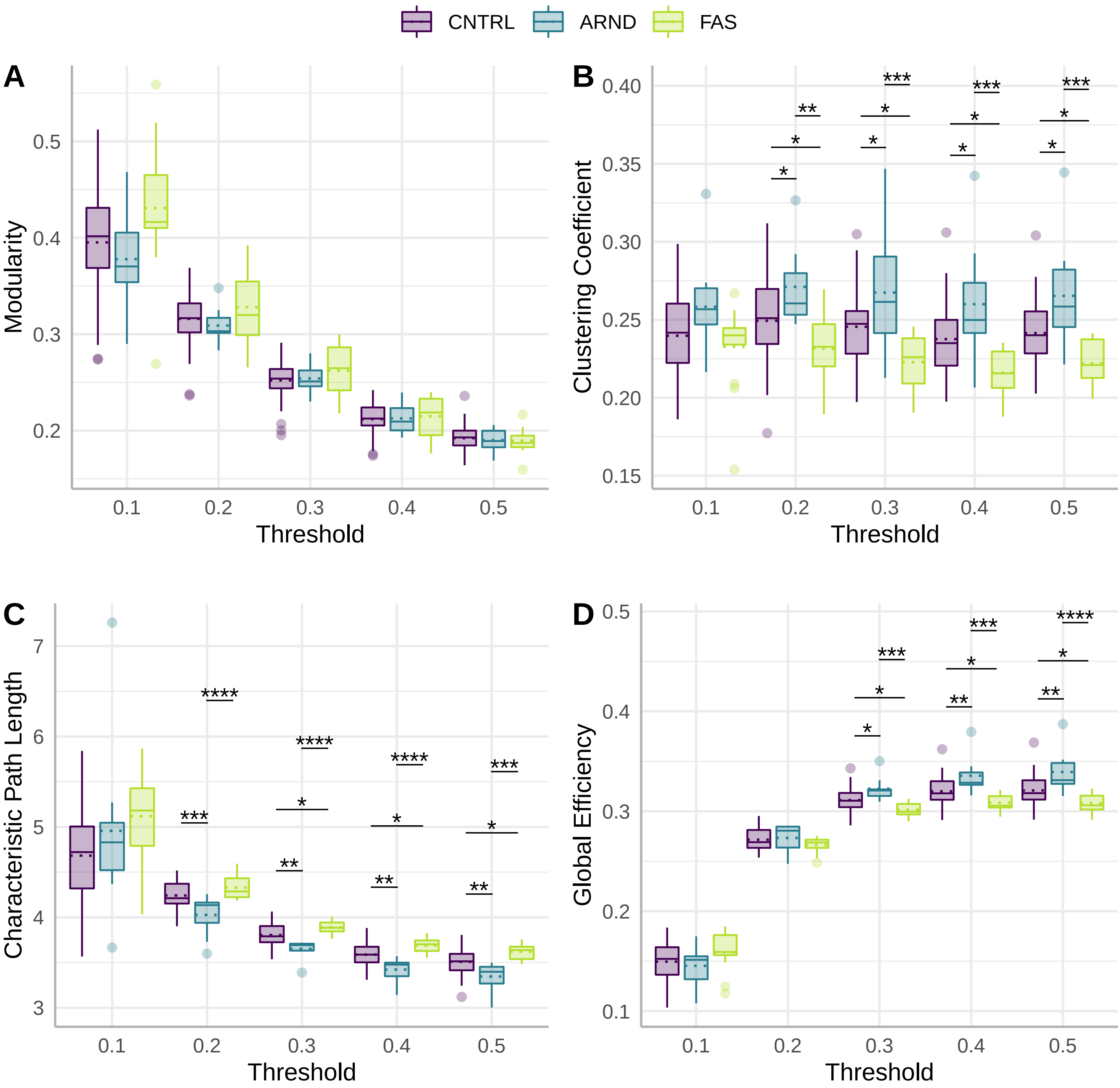
CNTRL
ARND
FAS
A
Modularity
Threshold
B
Clustering Coefficient
Threshold
C
Characteristic Path Length
Threshold
D
Global Efficiency
Threshold

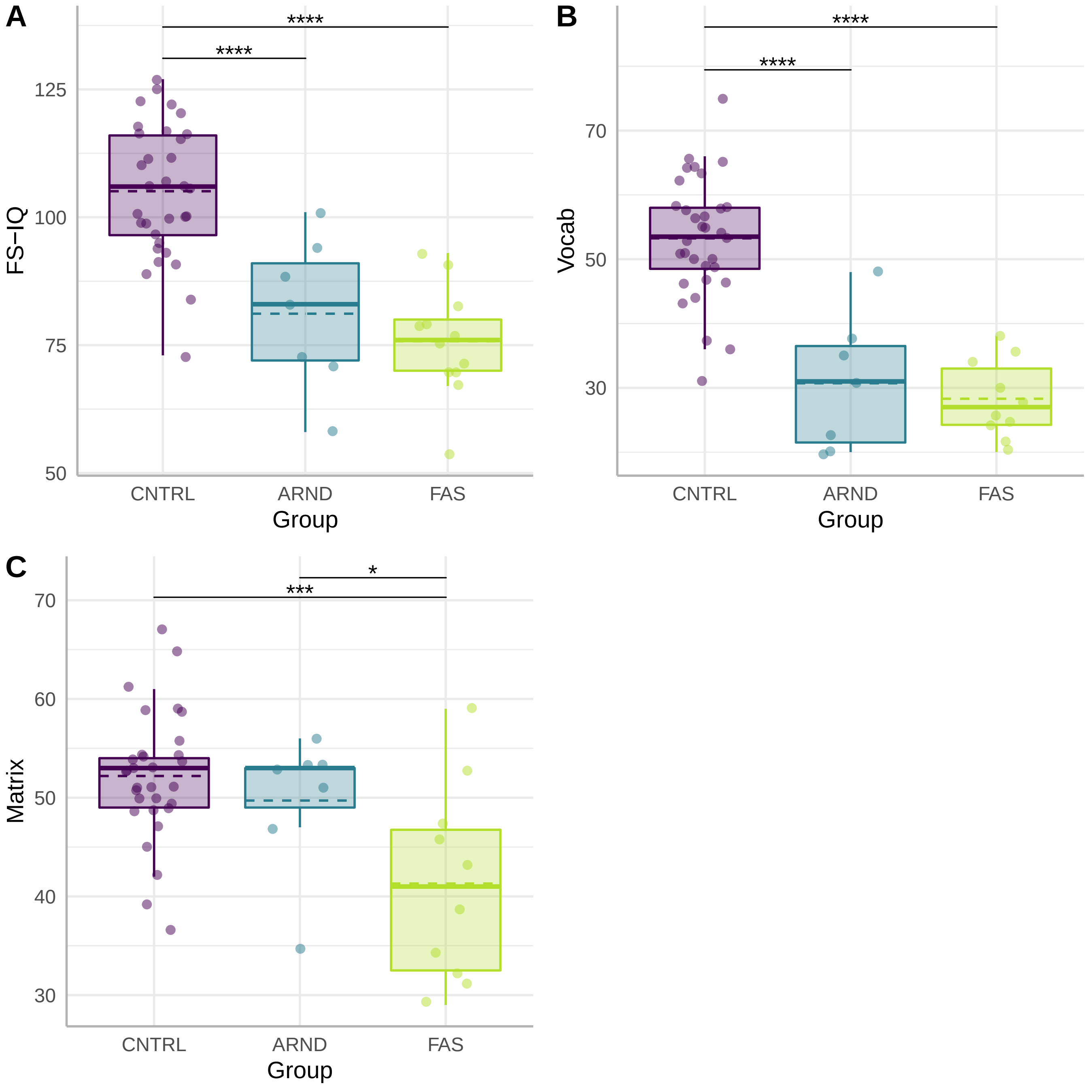

A
FS−IQ
125
100
75
50
****
****
CNTRL
ARND
FAS
Group
B
Vocab
70
50
30
****
****
CNTRL
ARND
FAS
Group
C
Matrix
70
60
50
40
30
*
***
CNTRL
ARND
FAS
Group

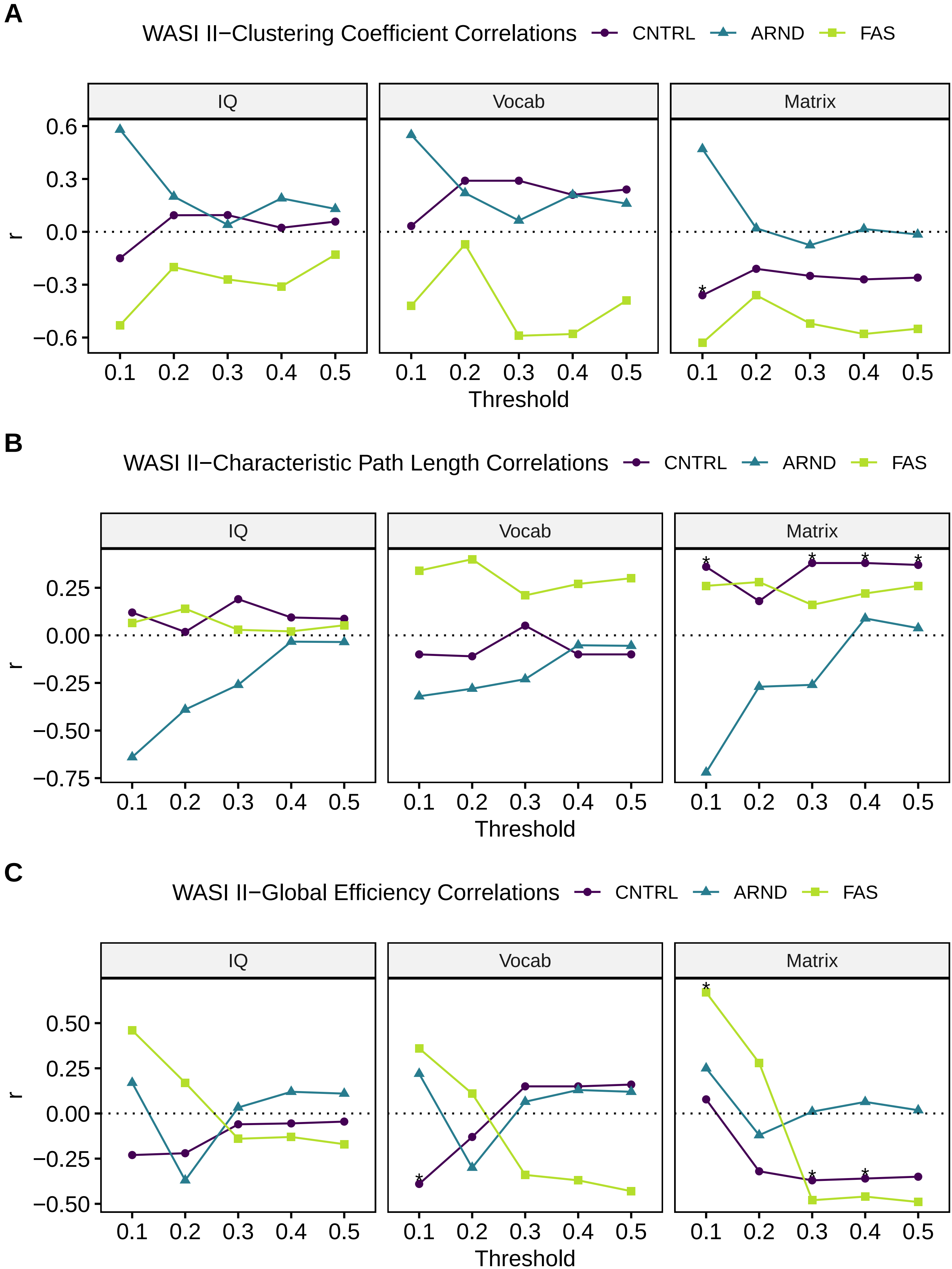

A
WASI II−Clustering Coefficient Correlations
CNTRL
ARND
FAS
IQ
Vocab
Matrix
r
Threshold
B
WASI II−Characteristic Path Length Correlations
CNTRL
ARND
FAS
IQ
Vocab
Matrix
r
Threshold
C
WASI II−Global Efficiency Correlations
CNTRL
ARND
FAS
IQ
Vocab
Matrix
r
Threshold

Supplementary Information

Supplementary Figure 1 – Retained Independent Components

Independent components (ICs) are shown in the sagittal, coronal, and axial planes corresponding to the peak component z-score value and thresholded to z = 2.4.

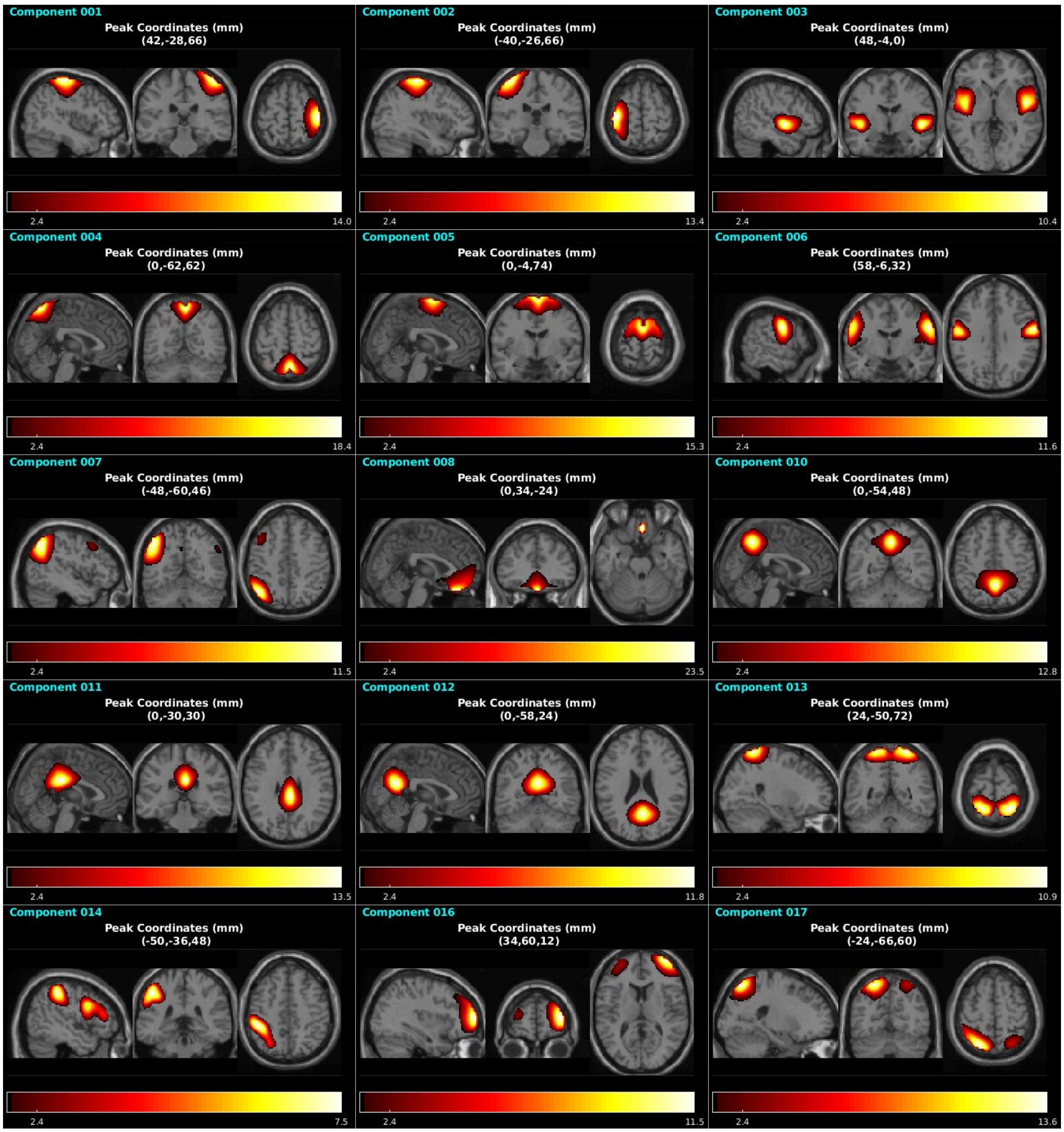

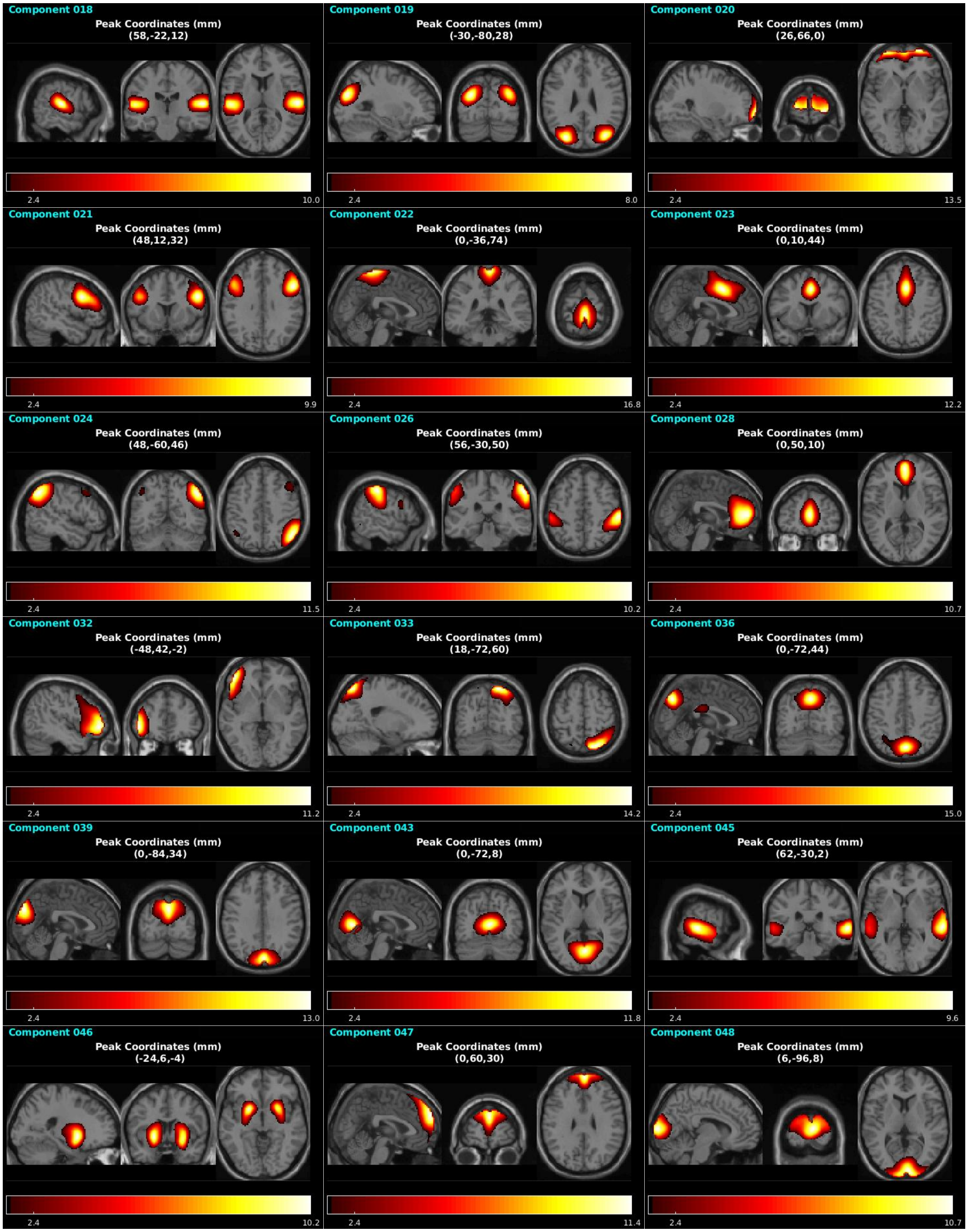

Component 018
Peak Coordinates (mm)
(58,-22,12)
2.4
10.0
Component 019
Peak Coordinates (mm)
(-30,-80,28)
2.4
8.0
Component 020
Peak Coordinates (mm)
(26,66,0)
2.4
13.5
Component 021
Peak Coordinates (mm)
(48,12,32)
2.4
9.9
Component 022
Peak Coordinates (mm)
(0,-36,74)
2.4
16.8
Component 023
Peak Coordinates (mm)
(0,10,44)
2.4
12.2
Component 024
Peak Coordinates (mm)
(48,-60,46)
2.4
11.5
Component 026
Peak Coordinates (mm)
(56,-30,50)
2.4
10.2
Component 028
Peak Coordinates (mm)
(0,50,10)
2.4
10.7
Component 032
Peak Coordinates (mm)
(-48,42,-2)
2.4
11.2
Component 033
Peak Coordinates (mm)
(18,-72,60)
2.4
14.2
Component 036
Peak Coordinates (mm)
(0,-72,44)
2.4
15.0
Component 039
Peak Coordinates (mm)
(0,-84,34)
2.4
13.0
Component 043
Peak Coordinates (mm)
(0,-72,8)
2.4
11.8
Component 045
Peak Coordinates (mm)
(62,-30,2)
2.4
9.6
Component 046
Peak Coordinates (mm)
(-24,6,-4)
2.4
10.2
Component 047
Peak Coordinates (mm)
(0,60,30)
2.4
11.4
Component 048
Peak Coordinates (mm)
(6,-96,8)
2.4
10.7

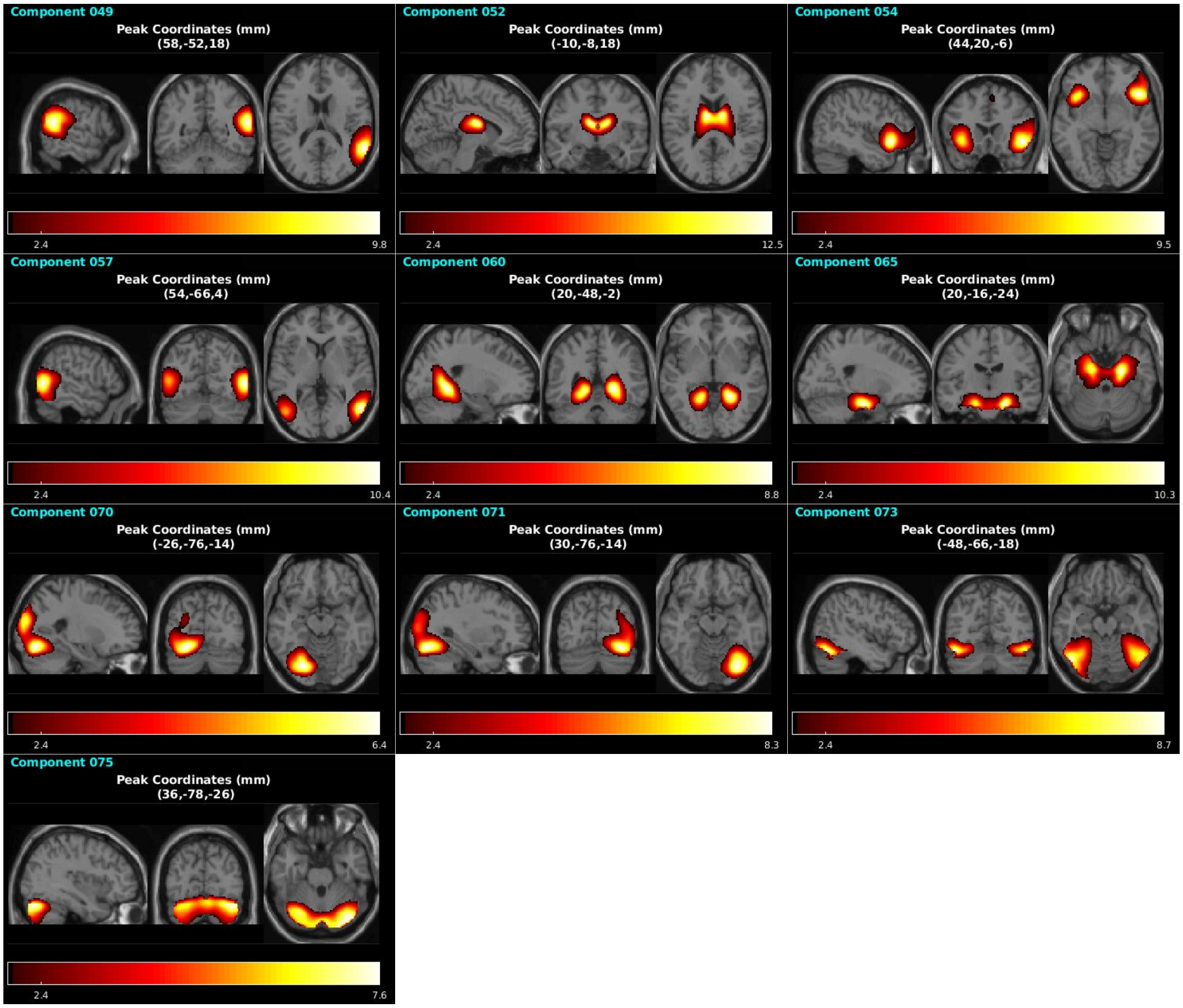
Component 049
Peak Coordinates (mm)
(58,-52,18)
2.4
9.8
Component 052
Peak Coordinates (mm)
(-10,-8,18)
2.4
12.5
Component 054
Peak Coordinates (mm)
(44,20,-6)
2.4
9.5
Component 057
Peak Coordinates (mm)
(54,-66,4)
2.4
10.4
Component 060
Peak Coordinates (mm)
(20,-48,-2)
2.4
8.8
Component 065
Peak Coordinates (mm)
(20,-16,-24)
2.4
10.3
Component 070
Peak Coordinates (mm)
(-26,-76,-14)
2.4
6.4
Component 071
Peak Coordinates (mm)
(30,-76,-14)
2.4
8.3
Component 073
Peak Coordinates (mm)
(-48,-66,-18)
2.4
8.7
Component 075
Peak Coordinates (mm)
(36,-78,-26)
2.4
7.6

Supplementary Table 1 – Component Coordinates and Anatomical Location

IC Number	Coordinates	Anatomical Location
1	42,-28,66	Right Postcentral Gyrus
2	-40,-26,66	Left Postcentral Gyrus
3	48,-4,0	Bilateral Insular Cortex
4	0,-62,62	Bilateral Precuneus, Midline
5	0,-4,74	Bilateral Supplementary Motor Area, Midline
6	58,-6,32	Bilateral Post Central Gyrus
7	-48,-60,46	Left Angular Gyrus, Precuneus, Right Angular Gyrus
8	0,34,-24	Bilateral Rectal Gyrus, Anterior Cingulate Cortex
10	0, -54,48	Bilateral Precuneus
11	0, -30,30	Bilateral Posterior Cingulate Cortex
12	0,-58,24	Bilateral Precuneus
13	24,-50,72	Bilateral Superior Parietal Lobule
14	-50,36,48	Left Inferior Parietal Lobule, Inferior Frontal Gyrus
16	34,60,12	Right Superior Frontal Gyrus
17	-24,-66,60	Left Superior Parietal Lobule
18	58,-22,12	Bilateral Superior Temporal Gyrus
19	-30,-80,28	Bilateral Occipital Gyrus
20	26,66,0	Bilateral Superior Frontal Gyrus, Anterior Cingulate Cortex
21	48,12,32	Bilateral Superior Frontal Gyrus
22	0,-36,74	Bilateral Paracentral Lobule
23	0,10,44	Bilateral Supplementary Motor Area
24	48,-60,46	Right Angular Gyrus
26	56,-30,50	Right Inferior Parietal Lobule, Supra Marginal Gyrus
28	0,50,10	Bilateral Anterior Cingulate Cortex
32	-48,42,-2	Left Inferior Frontal Gyrus
33	18,-72, 60	Right Superior Parietal Lobule
36	0,-72,44	Bilateral Precuneus, Posterior Cingulate Cortex
39	0,-84,34	Bilateral Cuneus
43	0,-72,8	Bilateral Lingual Gyrus
45	62,-30,2	Bilateral Middle and Superior Temporal Gyrus
46	-24,6,-4	Bilateral Basal Ganglia
47	0,60,30	Superior Medial Gyrus
48	6,-96,8	Bilateral Calcarine Gyrus
49	58,-52,18	Right Middle Temporal Gyrus
52	-10,-8,18	Bilateral Thalamus
54	44,20,-6	Bilateral Insular Cortex
57	54,-66,4	Bilateral Middle and Inferior Temporal Gyrus
60	20,-48,-2	Bilateral Lingual Gyrus
65	20,-16,-24	Bilateral Parahippocampal Gyrus
70	-26,-76,-14	Left Cerebellum
71	30,-76,-14	Right Cerebellum
73	-48,-66,-18,	Bilateral Cerebellum
75	36,-78,-26	Bilateral Cerebellum

Supplementary Figure 2 – Representation of peak IC values (nodes) in 3-dimensional space.

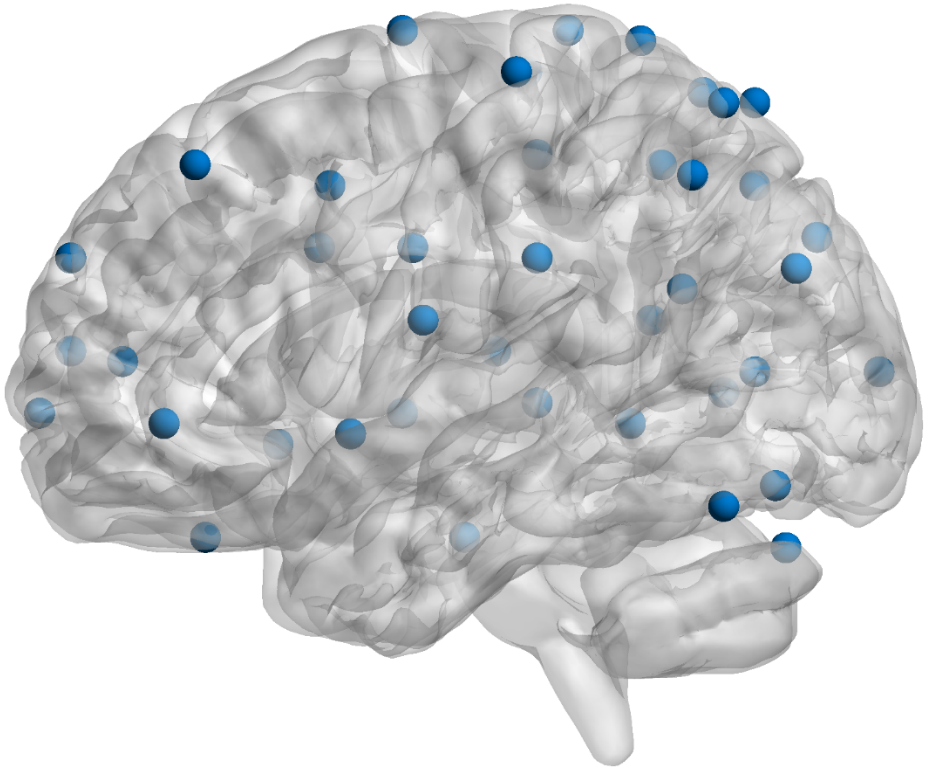

Supplementary Figure 3 – Boxplots and results of between-group comparisons on graph theory metrics within threshold. Solid horizontal lines within each box represent the median, while dotted lines represent the mean. Panel A) modularity; B) clustering coefficient, C) characteristic path length, D) global efficiency. CNTRL, controls; ARND, alcohol neurodevelopmental disorder, FAS, fetal alcohol syndrome. ****, p < 0.0001; ***, p < 0.001; **, p < 0.01; *, p < 0.05. All p values are corrected by Bonferroni method. For analyses of characteristic path length, one data point from a CNTRL participant at the 0.2 threshold was excluded as an outlier resulting in a sample size of n = 35 for that threshold only. All other remaining sample sizes were CNTRL = 36, ARND = 9, and FAS = 13.

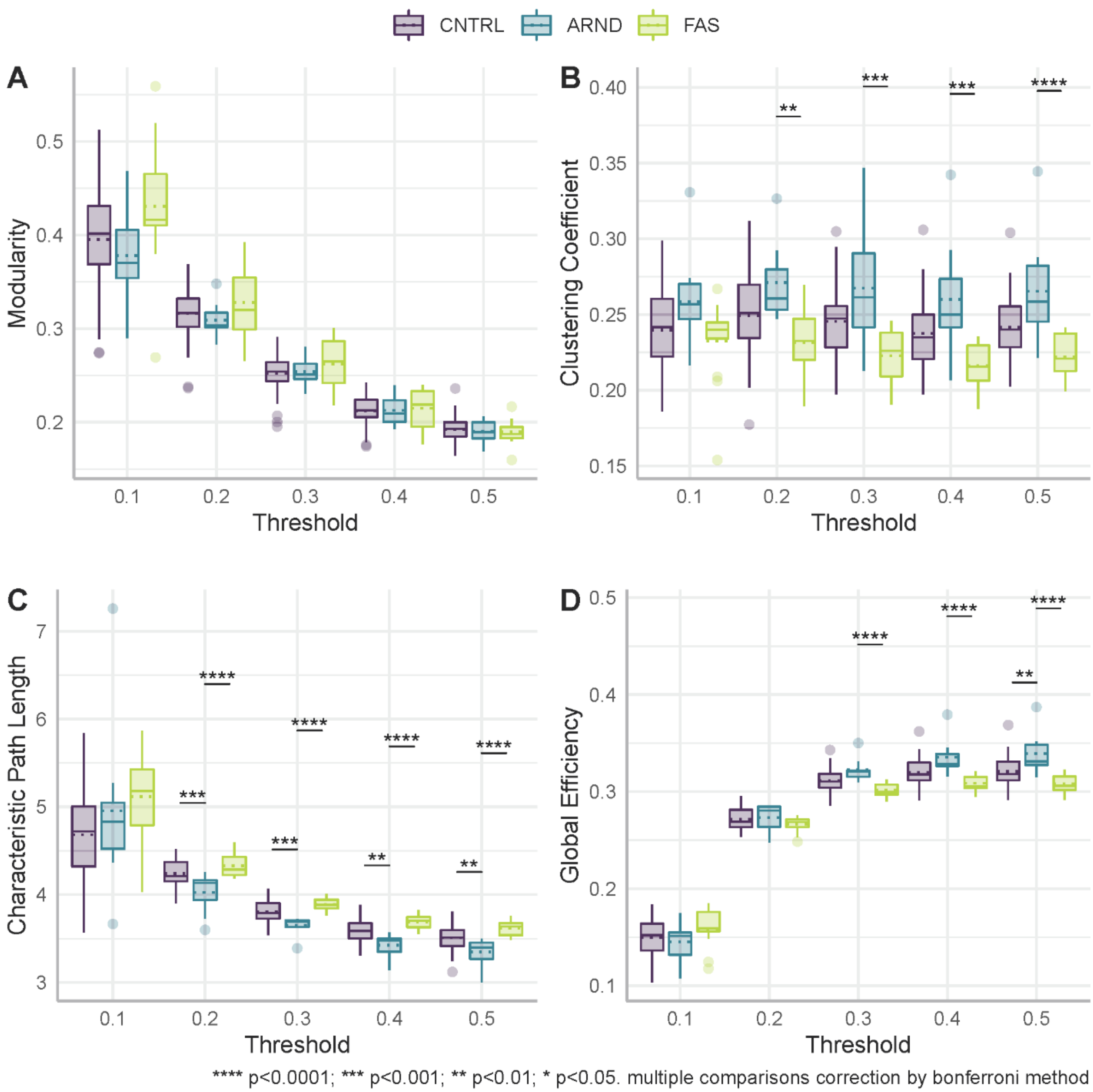

Supplementary Figure 4 – Boxplots and results of between-group comparisons on graph theory metrics within threshold. Solid horizontal lines within each box represent the median, while dotted lines represent the mean. Panel A) modularity; B) clustering coefficient, C) characteristic path length, D) global efficiency. CNTRL, controls; FASD, fetal alcohol spectrum disorder. ****, p < 0.0001; ***, p < 0.001; **, p < 0.01; *, p < 0.05. All p values are corrected by FDR method. For analyses of characteristic path length, one data point from a CNTRL participant at the 0.2 threshold was excluded as an outlier resulting in a sample size of n = 35 for that threshold only. All other remaining sample sizes were CNTRL = 36, FASD = 21.

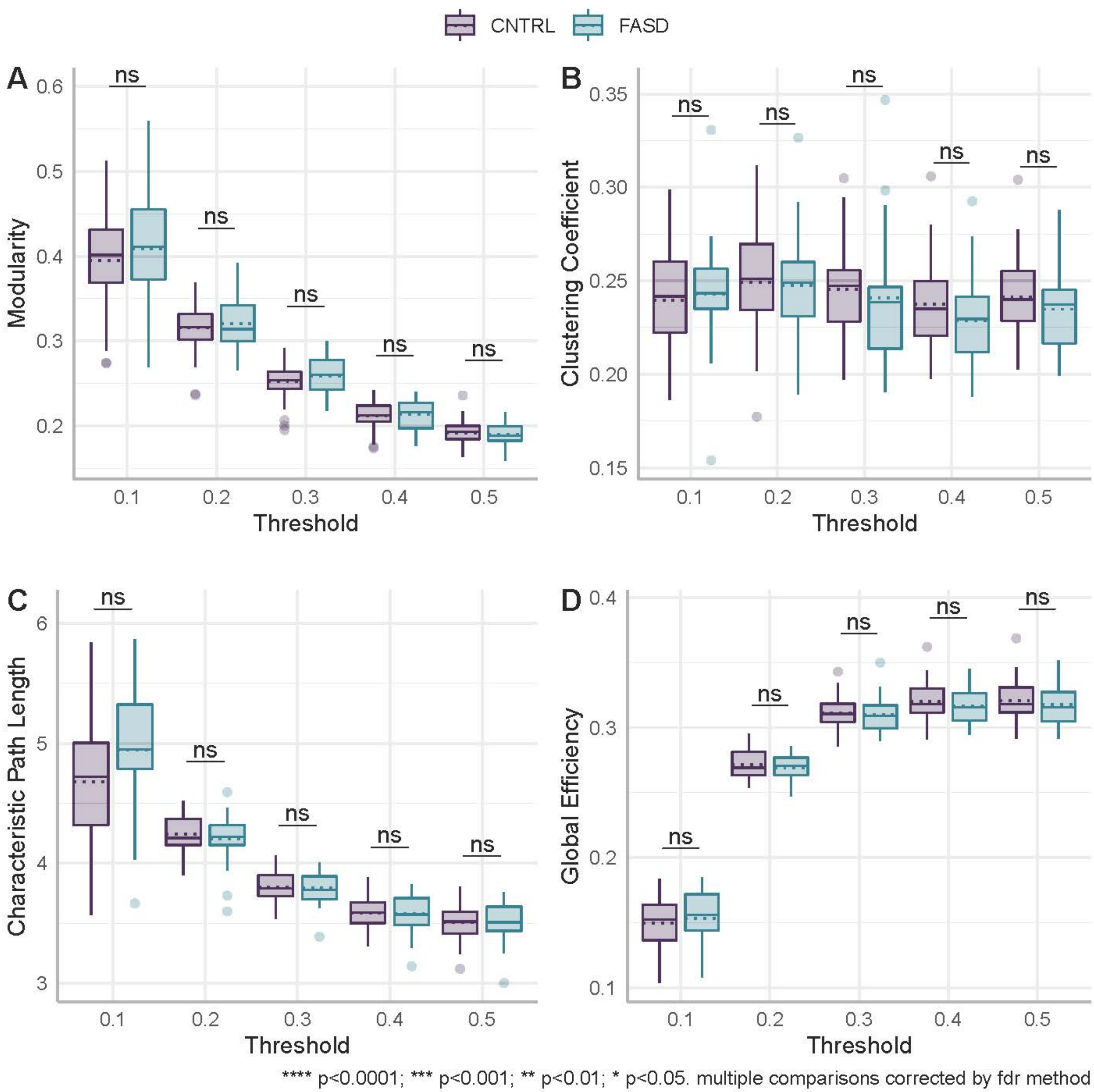

Supplementary Table 2 – Correlations between average clustering coefficient and WASI FS-IQ and subtest scores and p-values, and confidence intervals (CI).

Average Clustering Coefficient

Threshold	Group	WASI	r	P- value	CI Low	CI High
0.1	CNTRL	FS-IQ	-0.15	0.42	-0.47	0.21
0.2	CNTRL	FS-IQ	0.09	0.61	-0.26	0.43
0.3	CNTRL	FS-IQ	0.10	0.61	-0.26	0.43
0.4	CNTRL	FS-IQ	0.02	0.90	-0.33	0.37
0.5	CNTRL	FS-IQ	0.06	0.75	-0.30	0.40
0.1	ARND	FS-IQ	0.58	0.17	-0.30	0.93
0.2	ARND	FS-IQ	0.20	0.67	-0.65	0.83
0.3	ARND	FS-IQ	0.04	0.93	-0.74	0.77
0.4	ARND	FS-IQ	0.19	0.68	-0.66	0.83
0.5	ARND	FS-IQ	0.13	0.78	-0.69	0.80
0.1	FAS	FS-IQ	-0.53	0.08	-0.85	0.06
0.2	FAS	FS-IQ	-0.20	0.53	-0.70	0.42
0.3	FAS	FS-IQ	-0.27	0.39	-0.73	0.36
0.4	FAS	FS-IQ	-0.31	0.32	-0.75	0.32
0.5	FAS	FS-IQ	-0.13	0.69	-0.65	0.48
0.1	CNTRL	Vocab	0.03	0.86	-0.32	0.38
0.2	CNTRL	Vocab	0.29	0.11	-0.07	0.58
0.3	CNTRL	Vocab	0.29	0.11	-0.06	0.58
0.4	CNTRL	Vocab	0.21	0.25	-0.15	0.52
0.5	CNTRL	Vocab	0.24	0.18	-0.12	0.54
0.1	ARND	Vocab	0.55	0.20	-0.35	0.92
0.2	ARND	Vocab	0.22	0.64	-0.64	0.83
0.3	ARND	Vocab	0.06	0.89	-0.72	0.78
0.4	ARND	Vocab	0.21	0.65	-0.65	0.83
0.5	ARND	Vocab	0.16	0.73	-0.67	0.82
0.1	FAS	Vocab	-0.42	0.23	-0.83	0.29
0.2	FAS	Vocab	-0.07	0.85	-0.67	0.58
0.3	FAS	Vocab	-0.59	0.07	-0.89	0.06
0.4	FAS	Vocab	-0.58	0.08	-0.89	0.07
0.5	FAS	Vocab	-0.39	0.27	-0.82	0.32
0.1	CNTRL	Matrix	-0.36	0.05	-0.63	-0.01
0.2	CNTRL	Matrix	-0.21	0.27	-0.52	0.16
0.3	CNTRL	Matrix	-0.25	0.18	-0.55	0.12
0.4	CNTRL	Matrix	-0.27	0.14	-0.57	0.09
0.5	CNTRL	Matrix	-0.26	0.16	-0.56	0.10
0.1	ARND	Matrix	0.47	0.29	-0.44	0.90
0.2	ARND	Matrix	0.02	0.97	-0.74	0.76
0.3	ARND	Matrix	-0.08	0.87	-0.78	0.72
0.4	ARND	Matrix	0.02	0.97	-0.75	0.76
0.5	ARND	Matrix	-0.02	0.97	-0.76	0.75
0.1	FAS	Matrix	-0.63	0.05	-0.90	0.00

0.2	FAS	Matrix	-0.36	0.30	-0.81	0.35
0.3	FAS	Matrix	-0.52	0.12	-0.87	0.16
0.4	FAS	Matrix	-0.58	0.08	-0.88	0.08
0.5	FAS	Matrix	-0.55	0.10	-0.88	0.12

Supplementary Table 3 - Correlations between characteristic path length and WASI FS-IQ and subtest scores and p-values, and confidence intervals (CI).

Characteristic Path Length

Threshold	Group	WASI	r	P-value	CI Low	CI High
0.1	CNTRL	FS-IQ	0.12	0.52	-0.24	0.45
0.2	CNTRL	FS-IQ	0.02	0.92	-0.33	0.36
0.3	CNTRL	FS-IQ	0.19	0.29	-0.17	0.51
0.4	CNTRL	FS-IQ	0.09	0.61	-0.26	0.43
0.5	CNTRL	FS-IQ	0.09	0.64	-0.27	0.42
0.1	ARND	FS-IQ	-0.64	0.12	-0.94	0.22
0.2	ARND	FS-IQ	-0.39	0.39	-0.88	0.52
0.3	ARND	FS-IQ	-0.26	0.58	-0.85	0.62
0.4	ARND	FS-IQ	-0.03	0.94	-0.77	0.74
0.5	ARND	FS-IQ	-0.04	0.94	-0.77	0.74
0.1	FAS	FS-IQ	0.07	0.84	-0.53	0.62
0.2	FAS	FS-IQ	0.14	0.67	-0.47	0.66
0.3	FAS	FS-IQ	0.03	0.93	-0.55	0.59
0.4	FAS	FS-IQ	0.02	0.95	-0.56	0.59
0.5	FAS	FS-IQ	0.05	0.87	-0.54	0.61
0.1	CNTRL	Vocab	-0.10	0.57	-0.44	0.25
0.2	CNTRL	Vocab	-0.11	0.55	-0.44	0.25
0.3	CNTRL	Vocab	0.05	0.78	-0.30	0.39
0.4	CNTRL	Vocab	-0.10	0.59	-0.43	0.26
0.5	CNTRL	Vocab	-0.10	0.57	-0.44	0.25
0.1	ARND	Vocab	-0.32	0.48	-0.87	0.57
0.2	ARND	Vocab	-0.28	0.55	-0.85	0.60
0.3	ARND	Vocab	-0.23	0.62	-0.84	0.63
0.4	ARND	Vocab	-0.05	0.91	-0.77	0.73
0.5	ARND	Vocab	-0.06	0.91	-0.78	0.73
0.1	FAS	Vocab	0.34	0.33	-0.36	0.80
0.2	FAS	Vocab	0.40	0.26	-0.31	0.82
0.3	FAS	Vocab	0.21	0.57	-0.49	0.74
0.4	FAS	Vocab	0.27	0.45	-0.43	0.77
0.5	FAS	Vocab	0.30	0.41	-0.41	0.78
0.1	CNTRL	Matrix	0.36	0.05	0.01	0.63
0.2	CNTRL	Matrix	0.18	0.33	-0.18	0.50
0.3	CNTRL	Matrix	0.38	0.03	0.03	0.65
0.4	CNTRL	Matrix	0.38	0.04	0.03	0.65
0.5	CNTRL	Matrix	0.37	0.04	0.02	0.64

0.1	ARND	Matrix	-0.72	0.07	-0.96	0.07
0.2	ARND	Matrix	-0.27	0.56	-0.85	0.61
0.3	ARND	Matrix	-0.26	0.57	-0.85	0.61
0.4	ARND	Matrix	0.09	0.85	-0.71	0.79
0.5	ARND	Matrix	0.04	0.94	-0.74	0.77
0.1	FAS	Matrix	0.26	0.47	-0.44	0.76
0.2	FAS	Matrix	0.28	0.43	-0.42	0.77
0.3	FAS	Matrix	0.16	0.66	-0.52	0.72
0.4	FAS	Matrix	0.22	0.55	-0.48	0.74
0.5	FAS	Matrix	0.26	0.46	-0.44	0.77

Supplementary Table 4 - Correlations between global efficiency and WASI FS-IQ and subtest scores and p-values, and confidence intervals (CI).

Global Efficiency

Threshold	Group	WASI	r	p-value	CI Low	CI High
0.1	CNTRL	FS-IQ	-0.23	0.21	-0.53	0.13
0.2	CNTRL	FS-IQ	-0.22	0.23	-0.53	0.14
0.3	CNTRL	FS-IQ	-0.06	0.75	-0.40	0.30
0.4	CNTRL	FS-IQ	-0.06	0.76	-0.40	0.30
0.5	CNTRL	FS-IQ	-0.05	0.81	-0.39	0.31
0.1	ARND	FS-IQ	0.17	0.71	-0.67	0.82
0.2	ARND	FS-IQ	-0.37	0.41	-0.88	0.53
0.3	ARND	FS-IQ	0.03	0.94	-0.74	0.77
0.4	ARND	FS-IQ	0.12	0.79	-0.69	0.80
0.5	ARND	FS-IQ	0.11	0.81	-0.70	0.80
0.1	FAS	FS-IQ	0.46	0.13	-0.15	0.82
0.2	FAS	FS-IQ	0.17	0.59	-0.44	0.68
0.3	FAS	FS-IQ	-0.14	0.67	-0.66	0.47
0.4	FAS	FS-IQ	-0.13	0.68	-0.66	0.48
0.5	FAS	FS-IQ	-0.17	0.60	-0.68	0.45
0.1	CNTRL	Vocab	-0.39	0.03	-0.65	-0.05
0.2	CNTRL	Vocab	-0.13	0.47	-0.46	0.23
0.3	CNTRL	Vocab	0.15	0.43	-0.21	0.47
0.4	CNTRL	Vocab	0.15	0.42	-0.21	0.47
0.5	CNTRL	Vocab	0.16	0.38	-0.20	0.48
0.1	ARND	Vocab	0.22	0.64	-0.64	0.83
0.2	ARND	Vocab	-0.30	0.51	-0.86	0.58
0.3	ARND	Vocab	0.07	0.89	-0.72	0.78
0.4	ARND	Vocab	0.13	0.77	-0.69	0.81
0.5	ARND	Vocab	0.12	0.80	-0.70	0.80
0.1	FAS	Vocab	0.36	0.30	-0.35	0.81
0.2	FAS	Vocab	0.11	0.77	-0.56	0.69
0.3	FAS	Vocab	-0.34	0.33	-0.80	0.37
0.4	FAS	Vocab	-0.37	0.29	-0.81	0.34

0.5	FAS	Vocab	-0.43	0.22	-0.83	0.28
0.1	CNTRL	Matrix	0.08	0.68	-0.28	0.42
0.2	CNTRL	Matrix	-0.32	0.08	-0.61	0.03
0.3	CNTRL	Matrix	-0.37	0.04	-0.64	-0.02
0.4	CNTRL	Matrix	-0.36	0.05	-0.63	-0.01
0.5	CNTRL	Matrix	-0.35	0.05	-0.63	0.00
0.1	ARND	Matrix	0.25	0.59	-0.62	0.84
0.2	ARND	Matrix	-0.12	0.80	-0.80	0.70
0.3	ARND	Matrix	0.01	0.98	-0.75	0.76
0.4	ARND	Matrix	0.06	0.89	-0.72	0.78
0.5	ARND	Matrix	0.02	0.97	-0.75	0.76
0.1	FAS	Matrix	0.67	0.03	0.08	0.92
0.2	FAS	Matrix	0.28	0.43	-0.42	0.77
0.3	FAS	Matrix	-0.48	0.16	-0.85	0.21
0.4	FAS	Matrix	-0.46	0.18	-0.85	0.23
0.5	FAS	Matrix	-0.49	0.15	-0.86	0.20